The Pennsylvania State University

The Graduate School

Department of Chemical Engineering

MICROSTRUCTURAL CONTROL OF POLYARYLETHERKETONES

AND THEIR FIBER REINFORCED COMPOSITES

A Thesis in

Chemical Engineering

by

Dustin Veazey

Submitted in Partial Fulfillment
of the Requirements
for the Degree of

Master of Science

December 2018

The thesis of Dustin Veazey was reviewed and approved* by the following:

Enrique Gomez
Professor of Chemical Engineering and Materials Science
Thesis Advisor

Michael Hickner
Professor of Materials Science and Engineering, Chemistry and Chemical
    Engineering

Michael Janik
Professor of Chemical Engineering

Phillip Savage
Professor of Chemical Engineering
Head of the Department of Chemical Engineering

*Signatures are on file in the Graduate School

ABSTRACT

Interest in polyaryletherketones (PAEKs) and their carbon fiber reinforced composites continues to grow, and is driven by their increasing use in critical, high performance applications. Though these materials have seen widespread use in oil and gas, aerospace, medical and transportation industries, applications are currently limited by the thermal and mechanical properties of available PAEK polymer chemistries. The theme of this Master's thesis is the improvement of PAEK properties through control of the polymer microstructure. It includes a review of state of the art PAEK polymer chemistries, mechanical properties of their carbon fiber reinforced composites, and interfacial engineering techniques used to improve the fiber-matrix interfacial bond strength.

The original research presented is aimed at improving the high temperature steam resistance of PAEKs through covalent crosslinking and control of the crystalline microstructure. The effect of high temperature steam on the crystallinity and mechanical properties of existing PEEK and PEKK(T/I) polymers is investigated in order to aid design of more effective PAEK materials for high temperature steam applications. DSC, WAXD and DMA experiments show these materials undergo significant crystallization and reorganization after prolonged exposure to steam and suffer from embrittlement. Xanthydrol-based crosslinks are used to stabilize the PEKK crystal structure in order to prevent steam-assisted crystallization. Mechanical tests demonstrate the ductility is preserved for longer exposures to steam compared to neat PEKK, while DSC and WAXD data indicate xanthydrol crosslinks effectively stabilize the crystal structure against steam-assisted crystallization.

TABLE OF CONTENTS

LIST OF FIGURES

LIST OF TABLES

LIST OF EQUATIONS

ACKNOWLEDGEMENTS

Chapter 1

Introduction

1.1 Motivation and Thesis Overview

Polyaryletherkeotne (PAEK) polymers and their composites are increasingly utilized for high performance applications. For example, the demand for reduced transportation fuel consumption is driving a movement toward weight reduction in aerospace and automotive structures where aluminum and titanium alloys traditionally dominate. The desired light-weighting can be partially achieved through the adoption of carbon reinforced PAEKs as the material of construction for components previously made from metals. In order to be a true replacement for metal, however, PAEK composites must exhibit good mechanical properties, service lifetime and meet manufacturing cost requirements. This is also true of PAEKs used for critical applications in other industries, such as medical and oil and gas.

The underlying motivation for this thesis is the property improvement of PAEK thermoplastics and their carbon fiber composites through control of their microstructure. Similar to other polymers, the microstructure of PAEKs plays a significant role in their properties, behavior and performance. This work demonstrates that the microstructure can be tuned through a combination of state-of-the-art chemical modification techniques and processing methods in order to obtain enabling properties best suited for the given application.

Chapter 1 contains a summary of PAEK polymer synthesis and chemical modification techniques which is crucial background knowledge for subsequent chapters related to microstructural control. This includes a discussion of historical and cutting-edge PAEK

polymerization chemistry, PAEK copolymer properties and applications and recent methods for crosslinking PAEKs.

Chapter 2 is a comprehensive literature review and roadmap for PAEK carbon fiber reinforced composites. It illustrates the current landscape of PAEK composites, including properties, applications and manufacturing techniques. It also provides a brief explanation of micromechanical theory for fiber reinforced polymers and identifies the key material design parameters, such as critical fiber length and interfacial shear strength. The focus is on interfacial engineering to improve the polymer-fiber interfacial bond and the bulk composite properties. The most prevalent interfacial modification techniques are introduced and it highlights noteworthy examples from recent literature. Finally, it presents a future state for these composite materials and proposes that it can be achieved through improvements in the polymer-fiber interfacial bond.

Chapter 3 contains original research which seeks (1) to understand the effect of high temperature steam on the microstructure and mechanical properties of various PAEKs and (2) to enhance the mechanical performance of PEKKs for high temperature steam applications through crosslinking and control of the semicrystalline microstructure.

Chapter 4 summarizes the key points of the original work presented in this thesis and makes recommendations for future work to drive the continual improvement of PAEK polymers and composites.

1.2 PAEK Synthesis and Modification Chemistry

1.2.1 Polymerization

There are multiple routes available to synthesize PAEKs depending on the desired properties and functionality of the final polymer. Figure 1-1 illustrates polymerization schemes and highlights each route discussed here, but more comprehensive reviews are available.[1, 2] The

(a) Friedel-Crafts acylation

(b) Nucleophilic substitution

(c) Aryl chloride coupling

EK = aryl ether ketone

(d) Aryl amination

R₁ = CO, OC-Ar-CO R₂ = O, O-Ar-O
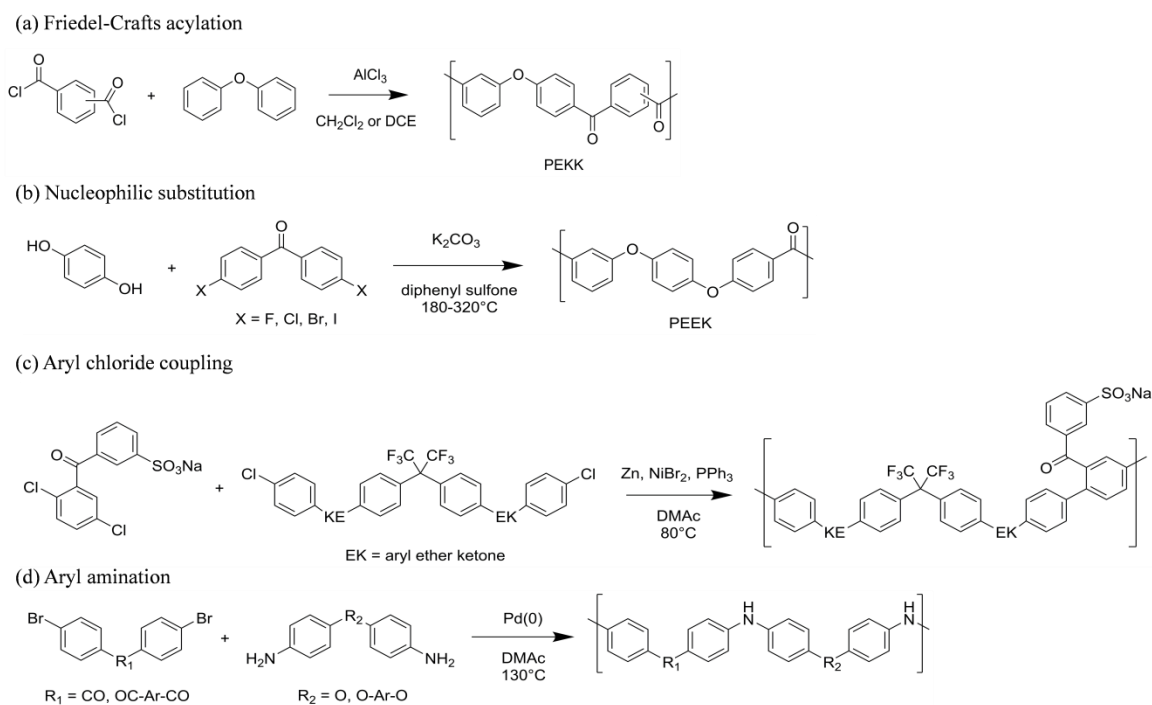
Figure 1-1: Polymerization routes for various PAEKs.

first route is electrophilic polycondensation in which Friedel-Crafts acylation occurs between a phenyl ether and an aromatic acid chloride using a Lewis acid catalyst at low temperature to minimize side reactions (Figure 1-1(a)).[3, 4] PEKK is commonly synthesized by this route from diphenyl ether and phthaloyl chloride in the presence of an aluminum chloride catalyst. Polymerization of high molecular weight products requires the use of organic solvents, such as 1,2-dichloroethane or methylene chloride, high temperature polymerization conditions to solubilize the growing polymer chains, and catalysts that are stable at high temperatures.

Another route is nucleophilic substitution of aromatic dihaloketones by diphenols (Figure 1-1(b)).[5] The extent of this reaction is largely dependent on the solvent conditions. This is the most common route to synthesize PEEK from difluorobenzophenone and bisphenol hydroquinone in diphenylsulfone as the solvent with a potassium carbonate catalyst at 180 to 320°C.

Organometallic-catalyzed polymerization routes are also available for PAEK synthesis, though these methods are limited to the synthesis of amorphous PAEKs. A series of sulfonated poly(*p*-phenylene-co-aryl ether ketone) copolymers for fuel cell membrane applications were prepared from coupling of aryl dichlorides using a Ni(0) catalyst (Figure 1-1(c)).[6] Higher molecular weights were obtained by improving solubility of the formed polymer by incorporating trifluoromethyl groups into the starting monomers, which also facilitated solution casting of membrane films.

A polyether ketone containing amine linkages in the main chain was synthesized via Pd(0) catalyzed aryl amination of dibromo ketone with aromatic ether diamine (Figure 1-1(d)).[7] The same polycondensation can also be achieved with a CuI homogeneous catalyst and a CuO nanocatalyst.[8] The resulting polymers have a T_g between 175-200°C and exhibit strong photoluminescence as well as mechanical strength; this polyether ketone may be ideally suited for light-emitting polymer applications. The aforementioned synthetic route has the benefit of lower reaction temperatures compared to traditional nucleophilic aromatic substitution polycondensations. Nevertheless, the resulting PAEKs must be soluble in the reaction media in order to obtain a high molecular weight product with good mechanical properties. Consequently, these polymers are amorphous and lack the chemical resistance of their semi-crystalline counterparts.

1.2.2 Copolymers

PAEK copolymers are attractive because they impart additional properties, such as increased T_g, greater solubility in organic solvents, lower dielectric constant, and lower water absorption, into a chemically and thermally stable PAEK chain structure. Most often, novel monomers intended to impart desired characteristics into the copolymer are synthesized, then

copolymerized using one of the above mentioned routes. The possibilities for different copolymer combinations are seemingly endless and are only limited by the imagination and available synthetic chemistry. The following recent examples, summarized in Figure 1-2, demonstrate the versatility of PAEK synthetic routes and the diversity of available copolymers and tailored monomers, as well as their effect on polymer properties.

A series of PEKKs containing imide moieties (Figure 1-2(a)) were prepared by Friedel-Crafts polycondensation over a wide range of molar ratios.[9] The copolymers containing 0-40 mol% of the imide linkage are semi-crystalline with T_g and T_m ranging from 170-183°C and 384-341°C, respectively. They exhibit good thermal stability, mechanical strength and chemical resistance comparable to commercially available homopolymer PAEKs.

(a) PEKK copolymers with imide linkages

(b) Pendant groups to improve solubility

(c) Pendant groups to improve dielectric constant
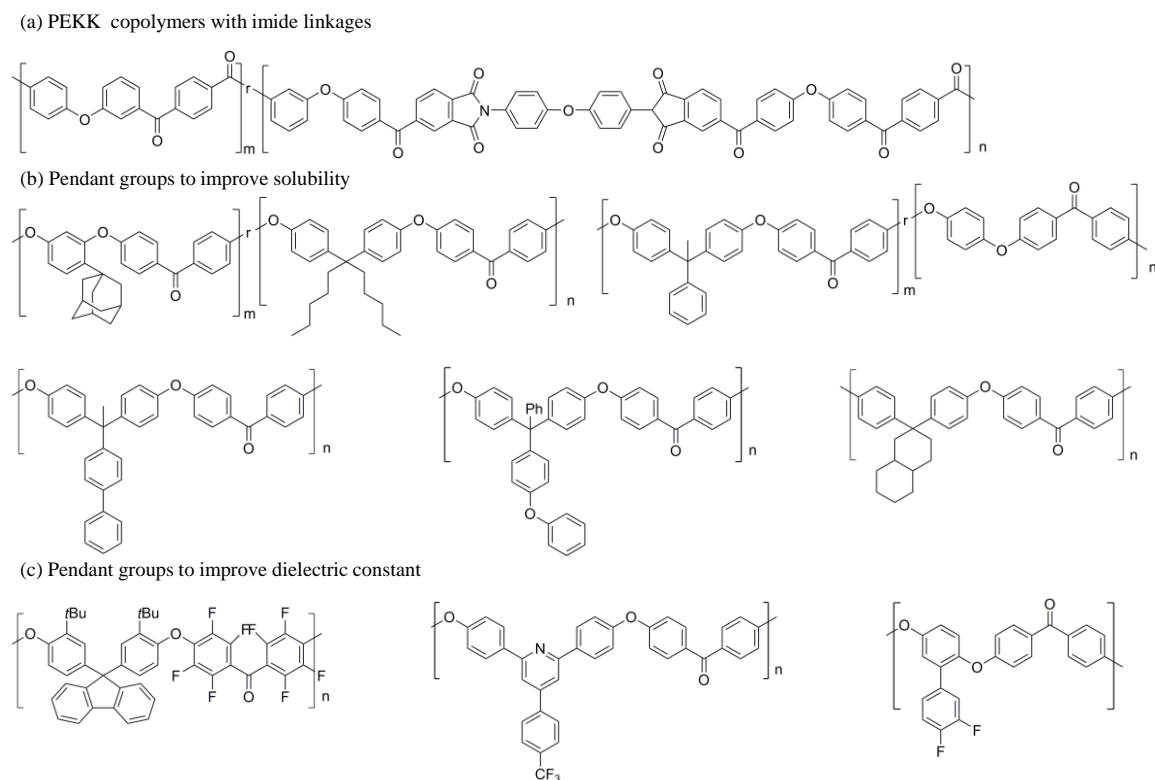
Figure 1-2: PAEK copolymers and tailored pendant groups to obtain desired enabling properties. (a) PEKK copolymer containing imide linkage to improve thermal resistance and mechanical properties at elevated temperature.[9] (b) Pendant groups to improve solubility for film casting from solution.[10-14] (c) Pendant groups to enhance the dielectric constant and hydrophobicity.[15-17]

Starting monomers may contain bulky pendent groups in order to increase the solubility of polymer chains in common organic solvents, thereby enabling solution casting of thin films. An added benefit is that higher molecular weights are achievable due to the improved solubility during polymerization of the growing polymer chain. Amorphous PEEK copolymers containing bulky pendent adamantyl and pentyl groups were synthesized by nucleophilic substitution under mild conditions (Figure 1-2(b)).[10] The mechanical moduli of these copolymers are at least half of commercially available PEEK, but the dielectric constants are lower and the polymers absorb less moisture. As a consequence, these copolymers are promising candidate materials as electrical insulators in microelectronic devices and gas separation membranes. Similarly, PEEK copolymers bearing pendent phenyl and methyl groups (Figure 1-2(b)) exhibit good solubility in organic solvents.[11]

A series of PEEKs and PEEKKs were synthesized with various degrees of methyl substitution on the aryl units and cardo decahydronaphthalene groups in the main chain (Figure 1-2(b)).[12] The intention was to disrupt chain packing and increase solubility in common organic solvents in order to facilitate solution processing of thin films. All polymers with cardo decahydronaphthalene groups were indeed amorphous and soluble in dichloromethane, chloroform, THF, pyridine and NMP at room temperature and could be cast into tough, flexible films from chloroform solutions. The T_g of these polymers ranged from 194°C for the least substituted PEEKK to 251°C for the most substituted PEEK.

Other PAEKs were synthesized with (4-phenoxyphenyl)triphenylmethane moieties in the main chain (Figure 1-2(b)).[14] The polymers have good solubility in organic solvents at room temperature and were successfully cast into films from solutions. T_g of these polymers range from 174-196°C and tensile properties are comparable to other amorphous PAEKs. Incorporation of naphthyl and biphenyl side chains (Figure 1-2(b)) into various PAEKs also increases T_g and allows the polymers to dissolve easily in organic solvents.[13]

Fluorene-based poly(aryl fluoroaryl ethers) bearing pendant *tert*-butyl groups were synthesized by nucleophilic substitution with the intent of application as dielectric materials or in gas separation membranes (Figure 1-2(c)).[15] The resulting polymer has a high T_g of 264°C, is soluble in common organic solvents and exhibits a low dielectric constant and low water uptake. This synthesis is noteworthy due to the stereochemical selectivity of the polycondensation. Even though the biphenyl monomer contained fluorine atoms at three different positions, the 4-4' positions are the most reactive due to electronic and steric factors.

Several PAEKs were prepared with 4-(4-trifluoromethylphenyl)pyridine moieties in the main chain (Figure 1-2(c)) in order to create a strong, low dielectric constant materials for printed circuit boards.[16] All polymers have comparable mechanical properties to PEEK and PEKK and exhibit lower water uptake, probably due to the presence of the pendant trifluoromethyl groups. Dielectric constants of these materials range from 2.62-2.75 at 1 MHz, which is one of the lowest reported for fluorine-substituted PAEKs.

PEEKs with greater hydrophobicity and better dielectric properties for microelectronic devices were prepared by nucleophilic substitution polycondensation of fluorophenyl and difluorophenyl hydroquinones with difluorobenzophenone (Figure 1-2(c)).[17] The contact angle of water for solution-cast films increases from 83.9° for PEEK to 90.3° and 98.4° for mono and difluorophenyl-substituted PEEKs, respectively. The dielectric constants of the fluorine containing PEEKs are as low as 2.75 at 1 MHz for difluorophenyl-PEEK, likely due to the disruption of chain packing. The tensile strength and modulus of films prepared from fluorophenyl-PEEKs range from 95.2-98.3 MPa and 3.06-2.74 MPa, respectively.

The examples highlighted here demonstrate the effective use of copolymerization to tune the properties of PAEKs. On-going work is likely to lead to new materials with properties beyond the current state-of-the-art, by taking advantage of the tremendous versatility of organic chemistry.

1.2.3 Crosslinking

Post-polymerization modification of commercially available PEEK and PEKK to obtain desired properties can avoid costly polymerization and purification of tailor-made monomers and copolymers. Desired properties include higher T_g, dimensional stability and creep resistance at high temperature. Their insolubility in common organic solvents[18] poses challenges for obtaining uniformly modified polymers, so chemical treatments are usually conducted on fine powders or reactor flake in the presence of a solvent swelling agent or typical polymerization solvents.

Crosslinkable PEEKs based on aromatic imine crosslinks were prepared by modifying commercially available PEKK (Victrex 151G) in molten diphenyl sulfone from 250-260°C.[19] Figure 1-3 shows imine linkages were introduced at 5 and 10% of the ketone positions using phenylene diamine and other aromatic diamines.[20] During subsequent hot-pressing of films and curing, the free amines formed more imine linkages to complete the crosslink network. Crosslinked PEEKs have improved creep resistance at high temperature and higher T_g compared to unmodified PEEK. Also, a rubbery plateau modulus is apparent above T_g from 200-400°C.

These types of "soft" elastomeric PAEKs are envisioned for high temperature, high pressure seals and connectors in corrosive environments due to their dimensional stability, chemical resistance[21], and mechanical properties at elevated temperatures.

Burgoyne and coworkers developed a series of diol crosslinkers based on 9-fluorenenone with various rigid and flexible arylene backbones (phenyl ether, naphthyl, anthracyl, biaryl, etc.).[22] In particular, a crosslinker containing a diphenyl ether backbone (Figure 1-3(b)) was mechanically blended with Victrex PEEK450 in a cryomill and hot-pressed into rectangular specimens at 400°C. The crosslinked network is thermally stable up to 400°C and the T_g of the base polymer increases from 151°C to 161°C. The crosslinking is hypothesized to occur by initial

hydroxyl dissociation from the crosslinker to form a carbocation that then undergoes Friedel-Crafts alkylation of the arylene backbone.

(a) Imine linkage
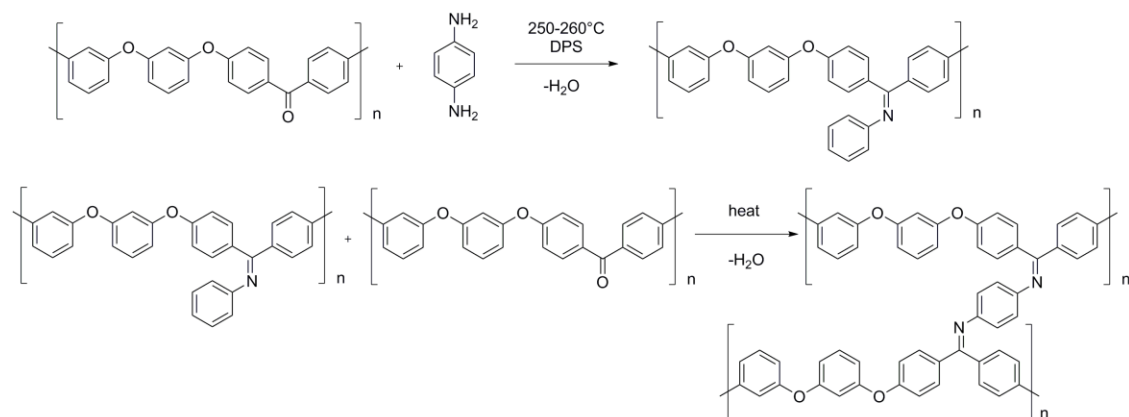
(b) Aryl linkage
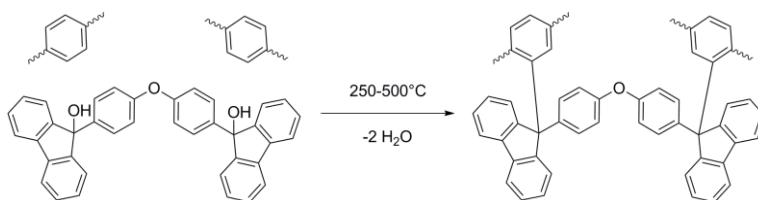
(c) Polyene/arylene linkage
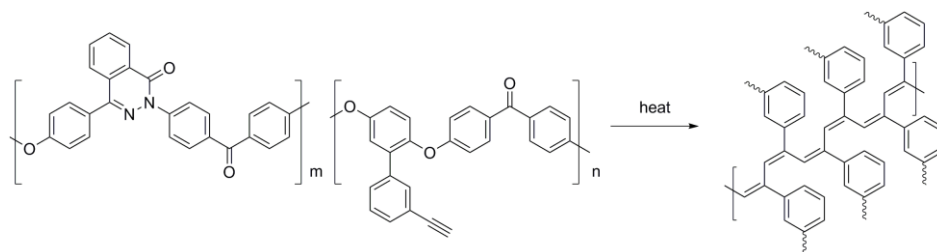
(d) S-triazine linkage
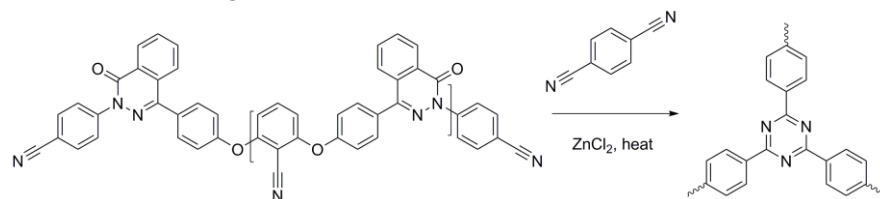
Figure 1-3: Recent crosslinking strategies for PAEKs.

A crosslinkable PPEK copolymer containing pendant ethynyl groups was prepared via nucleophilic substitution polycondensation with an ethynylphenyl bisphenol (Figure 1-3(c)).[23, 24] The ethynyl groups survive the polymer synthesis and undergo crosslinking at elevated temperatures, causing an increase in T_g to 266°C. Furthermore, the ethynyl groups were also modified by click chemistry to introduce fluorescent pyrene groups into the side chain, thereby increasing the photoemission quantum efficiency with respect to the unmodified PPEK copolymer.

A series of high T_g phthalazinone-based poly(arylene ether nitrile) oligomers bearing pendant and terminal cyano groups were synthesized by nucleophilic substitution.[25] The oligomers are crosslinkable in the presence of terephthalonitrile and zinc chloride catalyst above 300°C, resulting in the formation of s-triazine crosslinks as shown in Figure 1-3(d). The authors suggested that only the terminal cyano groups participate in the crosslinking via a trimerization mechanism. The crosslinked networks had gel contents ranging from 69-92wt% depending on the oligomer molecular weight, catalyst composition, curing time/temperature and concentration of crosslinkable groups.

The chemistries reported to date for crosslinking and modifying PAEKs in post-polymerization are promising for high temperature applications. Furthermore, these crosslinking chemistries can potentially be adapted to chemically modify the carbon fiber surface and improve bonding with PAEK matrices. This is critical to maximize the reinforcement efficiency of discontinuous carbon fiber composites, as we discuss below.

1.3 References

1. Shukla, D., Negi, Y. S., Sen Uppadhyaya, J. and Kumar, V. *Polymer Reviews* **2012**, *2*, 189-228.

2.   Pang, J. H., Zhang, H. B. and Jiang, Z. H. *Acta Polymerica Sinica* **2013**, *6*, 705-721.

3.   Rueda, D. R., Zolotukhin, M. G., Cagiao, M. E., Ania, F., Dosiere, M., Villers, D. and de Abajo, J. *Journal of Macromolecular Science-Physics* **2001**, *5*, 709-731.

4.   Zolotukhin, M. G., Rueda, D. R., Calleja, F. J. B., Cagiao, M. E., Bruix, M., Sedova, E. A. and Gileva, N. G. *Polymer* **1997**, *6*, 1471-1476.

5.   Attwood, T. E., Dawson, P. C., Freeman, J. L., Hoy, L. R. J., Rose, J. B. and Staniland, P. A. *Polymer* **1981**, *8*, 1096-1103.

6.   Zhang, X., Hu, Z. X., Pu, Y. L., Chen, S. S., Ling, J. N., Bi, H. P., Chen, S. W., Wang, L. J. and Okamoto, K. *Journal of Power Sources* **2012**, 261-268.

7.   Chang, G. J., Yang, L., Yang, J. X. and Lin, R. X. *Journal of Materials Science* **2014**, *20*, 7213-7220.

8.   Shang, Z. F., Yang, L. and Chang, G. J. *Macromolecular Research* **2015**, *10*, 937-943.

9.   Zhao, H., Xi, Q. and Cai, M. *Polymer Bulletin* **2011**, *7*, 1139-1152.

10.   Ba, J. Y., Geng, Z. and Mu, J. X. *Journal of Applied Polymer Science* **2013**, *1*, 193-200.

11.   Wu, T., Liu, P., Shi, M., Lu, J., Ye, G. and Xu, J. *Polymer International* **2011**, *9*, 1318-1323.

12.   Honkhambe, P. N., Pasale, S. K., Bhairamadgi, N. S., Kumbhar, K. P., Salunkhe, M. M. and Wadgaonkar, P. P. *Journal of Applied Polymer Science* **2011**, *3*, 1607-1613.

13.   Honkhambe, P. N., Dhamdhere, N. A., Tawade, B. V., Salunkhe, M. M. and Wadgaonkar, P. P. *High Performance Polymers* **2013**, *3*, 260-267.

14.   Li, X., Jiang, J. W., Yu, L. M., Liu, X. L. and Sheng, S. R. *High Performance Polymers* **2015**, *2*, 200-206.

15.   Wang, C. Y., Xu, C., Li, Q. F., Chen, W. T. and Zhao, X. Y. *Colloid and Polymer Science* **2015**, *1*, 313-318.

16.   Li, X., Liu, X. L., Cheng, L. J., Jiang, J. W. and Sheng, S. R. *Journal of Fluorine Chemistry* **2014**, 30-34.

17.   Xie, J., Peng, W.-y., Li, G. and Jiang, J.-m. *Polymer Bulletin* **2011**, *1*, 45-56.

18.   Browne, M. M., Forsyth, M. and Goodwin, A. A. *Polymer* **1997**, *6*, 1285-1290.

19.   Yurchenko, M. E., Huang, J. J., Robisson, A., McKinley, G. H. and Hammond, P. T. *Polymer* **2010**, *9*, 1914-1920.

20.   Tu, H. and Robisson, A. (Schlumberger Technology Corporation). U.S. Patent 8,436,106, May 7, 2013.

21. Hendrix, K., Van Eynde, M., Koeckelberghs, G. and Vankelecom, I. F. J. *Journal of Membrane Science* **2013**, 212-221.

22. Burgoyne, W. F. J., Nordquist, A. F., Drake, K. A. and Song, L. (Greene, Tweed & Co.). U.S. Patent 9,006,353, April 14, 2015.

23. He, Q. Z., Wang, J. Y., Zong, L. S., Liu, R. and Jian, X. G. *Polymer International* **2015**, *7*, 875-883.

24. Li, W. W., Tang, H. Y., Chen, X. F., Fan, X. H., Shen, Z. H. and Zhou, Q. F. *Polymer* **2008**, *19*, 4080-4086.

25. Yu, G., Liu, C., Wang, J., Li, G., Han, Y. and Jian, X. *Polymer* **2010**, *1*, 100-109.

Chapter 2

Next Generation High-Performance Carbon Fiber Thermoplastic

Composites Based on Polyaryletherketones

2.1 Introduction

Carbon fiber reinforced plastics are a versatile group of engineering composites that are currently employed in aerospace,[1-4] oil and gas,[5] medical,[6] and transportation applications[7]. They consist of thermoset or thermoplastic polymers reinforced with discontinuous, unidirectional or woven carbon fiber to obtain improved mechanical, thermal and electrical properties. Discontinuous refers to short and long carbon fiber composites that are typically manufactured via injection molding, compression molding, and extrusion. Continuous unidirectional composites contain carbon fiber that is both aligned and continuous throughout the composite form. Continuous fiber composites are also produced with fibers in cross-ply and woven orientations in order to obtain a composite with enhanced mechanical properties in multiple directions. The various architectures enable different applications. For example, discontinuous fiber composites are used in high-volume applications where nearly-isotropic mechanical properties are desirable. Continuous fiber composites are best utilized in low-volume applications that require maximal mechanical properties in one or two directions, such as impact panels, support beams and containment vessels.
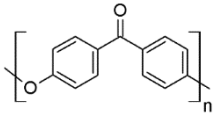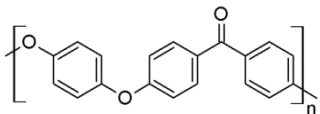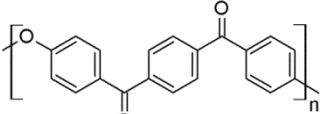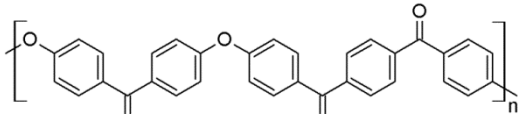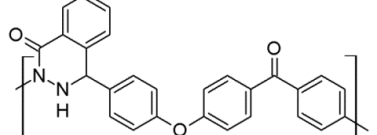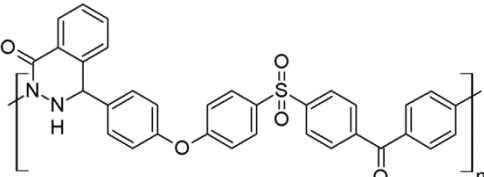
Many different types of natural (i.e. lignocellulosic[8, 9]) and synthetic (i.e. aramid[10, 11]) fibers are commercially available that are effective at reinforcing various plastics. Unterweger et al. provides an excellent overview of the mechanical and physical properties, cost, and reinforcement effectiveness of synthetic and thermoplastic reinforcing fibers in polymer matrices.[12] The advantages of carbon fiber compared to other synthetic fibers include high specific stiffness and strength, as well as good thermal and electrical conductivity. It is

commercially available in various strengths and stiffnesses at a much lower cost compared to other light-weight synthetic fibers. We focus on carbon fiber for this review, because we believe it will play a major role in the next generation of engineering materials for the reasons described above. The emerging market for carbon fiber reinforced plastics to replace metal components in high temperature and/or corrosive load bearing applications requires base polymers with good thermal stability and chemical resistance. Polyaryletherketones (PAEKs) are of great interest for higher temperature applications due to their inherent thermal stability and high glass transition temperature compared to other semicrystalline thermoplastics, such as polyamide 66[13], polyphenylene sulfide[14] and various fluoropolymers.[15-18] PAEKs exhibit excellent chemical resistance due to their chemistry and significant crystallinity; this class of materials also possess superior thermal stability,[19-21] hydrothermal and UV resistance,[22] and facile melt processability and recyclability[23] with carbon fiber.

Table 2-1 summarizes the chemical structure and thermal transitions of a variety of PAEKs. Polyether ether ketone (PEEK) is the most widely available and is often used for high pressure, high temperature applications despite having the lowest glass transition temperature in the PAEK family. Polyether ketone (PEK), polyether ketone ketone (PEKK) and polyether ketone ether ketone ketone (PEKEKK) have similar melt processabilities and crystallinity as PEEK, but can withstand slightly higher service temperatures due to their higher glass transition temperatures. Additionally, the crystallinity and thermal properties of PAEKs depend on their stereochemistry. For example, PEKK synthesized from terephthaloyl chloride (as shown in Table 2-1) exhibits a T_g of 175°C and T_m of 410°C with high crystallinity, while PEKK derived from isophthaloyl chloride exhibits a T_g of 156°C and T_m of 338°C with lower crystallinity. Consequently, a ratio of the two isomers (referred to as T/I ratio) is commonly used to balance high crystallinity and T_g with relatively low T_m to facilitate melt processability.

PAEKs that incorporate bulky monomers to restrict chain motion and therefore increase T_g have been reported. For example, polyphthalazinone ether sulfones exhibit glass transition temperatures ranging from 225 to 305°C depending on the phthalazinone/sulfone monomer

Table 2-1: Molecular structure and thermal transitions of select polyaryletherketones

Common name [abbrev.]	Molecular Structure	T_g (°C)	T_m (°C)	χ_c (%)
Poly(ether ketone) [PEK]		165[3]	373[3]	44[24]
Poly(ether ether ketone) [PEEK]		143[3]	340[3]	30[3]
Poly(ether ketone ketone) [PEKK]		175[3]	410[3]	35[3]
Poly(ether ketone ether ketone ketone) [PEKEKK]		169[25]	381[25]	30[26]
Poly(phthalazinone ether ketone) [PPEK]		253[27, 28]	NA	NA
Poly(phthalazinone ether sulfone ketone) [PPESK]		305[29]	NA	NA

ratio.[30] Similarly, polyphthalazinone ether ketone has a T_g of 253° C compared to 175°C for PEKK.[27, 28] Unfortunately, increasing the glass transition temperature by incorporating sterically bulky moieties in the main chain and as pendant groups can reduce the crystallinity, therefor limiting chemical and creep resistance. Nevertheless, a compromise between chemical resistance and high T_g can be achieved through copolymerization or melt blending.

The glass transition temperature of semi-crystalline PAEKs can be increased through copolymerization with the amorphous PAEKs mentioned previously.[31] These copolymers typically exhibit lower degree of crystallinity and slower crystallization rates than semi-crystalline PAEK, but improved chemical resistance compared to amorphous PAEKs. For example, PEEK-PPEK copolymers exhibit a T_g between 200 and 250°C.[32, 33] This allows access to higher service temperatures, while maintaining a reasonable degree of crystallinity and chemical resistance of neat PEKK. Similarly, co-polymers of polyphthalazinone ether sulfone ketone (PPESK) and PEKK exhibit glass transitions above 300°C.[29]

The combination of high strength, high modulus carbon fiber and high T_g PAEKs is a promising pathway to the next generation of polymer composite materials suited for high temperature applications in corrosive environments. Further progress will require the development of chemically resistant, high T_g PAEK blends and alloys and an improved engineering of interactions between PAEK and carbon fiber surfaces. We predict interfacial engineering of the inert carbon fiber surface for compatibility with the high T_g PAEK family will be required to unlock the full potential of this class of composites. In this review, we outline these challenges and present potential opportunities for the mechanical properties and interfacial engineering to move beyond current leading PAEK composites.

2.2 Mechanical Properties of PAEK-Carbon Fiber Composites

The mechanical properties of PAEK carbon fiber reinforced plastics generally depend on the form of the carbon fiber (unidirectional vs. discontinuous), its volume fraction and orientation in the composite matrix, and the manufacturing process (compression, injection, extrusion, etc.). Figure 2-1 compares typical tensile properties of PAEK-based carbon fiber reinforced plastics with common metal alloys. Unidirectional fiber composites comprising approximately 70 vol% carbon fiber exhibit superior tensile modulus and strength compared to metal alloys and represent the upper limit for mechanical properties of PAEK-based carbon fiber reinforced plastics because the carbon fiber is aligned continuously throughout. Unidirectional composites are usually assembled and compression molded in cross-ply layup patterns in order to achieve the high mechanical performance in more than one direction.[34] The mechanical properties of unidirectional and cross-ply composites are described by a simple rule of mixtures.
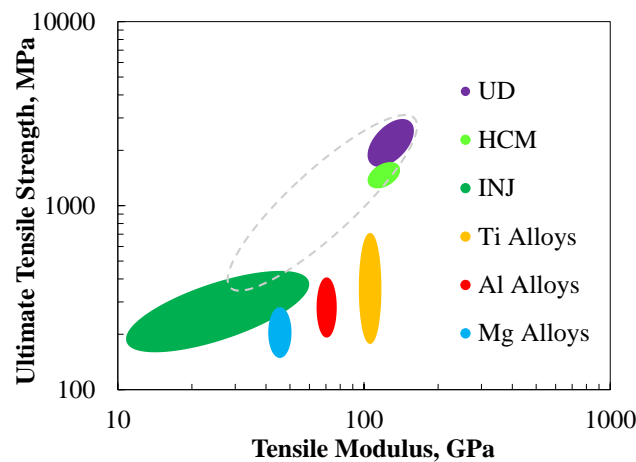
Figure 2-1: Typical tensile properties of common metallic alloys and carbon fiber reinforced PAEKs including continuous unidirectional fiber (UD), hot compression molded discontinuous fiber (HCM), injection molded short and long fiber composites (INJ). The region enclosed by the dotted line represents target properties for next generation PAEK carbon fiber reinforced composites that combine the mechanical properties of UD fibers and the processability of short fibers.

Processing parameters have a large influence on the final composite properties. For example, Price et al. demonstrated the relationship between thermoforming processing parameters (i.e. temperature and time) and final composite characteristics, such as crystallinity and surface roughness, for PPS carbon fiber laminates.[35] They found that the flexural strength of molded laminate composites is proportional to the degree of crystallinity of the thermoplastic matrix.

Additionally, the crystallinity of the matrix is controllable over a wide range and the desired crystallinity can be obtained by selecting the appropriate combination of mold tool temperature and processing time. Practically, a composite with high flexural strength would be produced by holding the mold at a temperature between T_g and T_c of the semi-crystalline thermoplastic matrix for a duration of time required to allow maximum crystallization to develop. A similar dependency is expected to exist for PAEK carbon fiber composites because they are also a high temperature semi-crystalline thermoplastic.

Compression molded discontinuous carbon fiber composites can have mechanical properties similar to unidirectional composites if the fibers are sufficiently long and aligned.[36-38] Unfortunately, the compression molding process applies low melt shear stress, which is insufficient for fiber alignment. Therefore, these composites are usually molded with randomly oriented fibers.

The mechanical properties of discontinuous short carbon fiber injection molded composites with high carbon fiber content can be comparable to low strength metal alloys, but are considerably lower than both continuous unidirectional and discontinuous compression molded composites. This drastic difference is characteristic of injection molded composites where high shear stresses in the polymer melt during processing promote fiber breakage. Because PAEKs are some of the more viscous thermoplastics, it is challenging to reduce melt shear stress and improve fiber length retention simply by adjusting processing conditions and mold design.

A popular strategy to overcome fiber breakage is to directly inject long pellets that consist of fiber bundles impregnated with polymer. The fibers span the full length of the pellet and can be up to 25 mm in length. Long fiber pellets of this type can be compression molded for small quantity parts that require high dimensional stability, stiffness and strength. They can also be injection molded in larger quantities to obtain high dimensional stability and reasonable stiffness and strength. Although fiber breakage still occurs in injection molded long fiber pellets, the fiber length is longer in the final part compared to compounded short fiber pellets. Phelps et al. predicted fiber length attrition in injection molding long fiber composites and verified their predictions in glass fiber/polypropylene long fiber composites.[39] They found that the fiber length decreased from an initial fiber length of 13 mm to a number average of 1.58 mm during injection molding. Despite the large decrease in fiber length, this is still a significant improvement over short glass fiber composites where the average fiber length is less than 0.4 mm after twin screw compounding.[40] Long fiber composites based on polypropylene[41-43] and polyamide[44-46] matrices are well covered in the literature, but PAEK matrices are largely unexplored due to their higher cost and processing challenges.

Processing challenges for PAEK-carbon fiber composite parts include high melt temperature and melt viscosity. Commercial PAEKs are available in various grades whose viscosities range approximately 100-1500 Pa·s at 370-400°C.[47-49] The high melt viscosity prevents composites from achieving full wet out or coverage of carbon fibers by the PAEK matrix, resulting in voids within the composite structure and reduced mechanical properties. Recommended composite processing temperatures are typically 50-80°F above the PAEK melting temperature to improve flow and ensure wet-out of fibers. The viscosity of the melt can also be reduced through the addition of compatible plasticizers, such as thermotropic liquid crystalline polymers and macrocyclic compounds, and thereby reduce the required processing temperatures. For example, addition of thermotropic liquid crystalline poly(ether ketone)acrylates

to PEEK reduced the melt viscosity and allowed the polymer to be processed at 365°C, which is lower than the required temperature for neat PEEK (380°C).[50] Similarly, temporary four-fold reduction of viscosity for PEEK was achieved by melt blending with macrocyclic aromatic thioetherketones.[51] But, the low molecular weight macrocycles underwent rapid uncatalyzed ring-opening polymerization above 430°C to form high molecular weight poly(thioetherketone), which restored the viscosity to that of neat PEEK. This strategy could facilitate full wet out of carbon fiber bundles and aid processing of composite parts, while preserving the PAEK matrix properties. At least one commercial disadvantage, however, is the additional high temperature ring-opening polymerization step, which is similar to curing required for thermoset based carbon fiber composites.

Continuous fiber composite parts are manufactured from woven, nonwoven and unidirectional prepreg fabrics and sheet molding compounds (SMCs), as well as impregnated carbon fiber tows and tapes (towpregs). Processing techniques for continuous fiber composites include in and out of autoclave compression molding, thermostamping, thermoforming, filament winding, automated fiber placement and 3-D printing. Discontinuous fiber composites are typically manufactured from bulk molding compounds (BMCs) via compression molding and from long fiber pellets via injection molding. In all cases, full fiber wet out is essential to obtain good mechanical properties.

Many micromechanical models have been developed and adapted to predict the macromechanical behavior of discontinuous carbon fiber reinforced plastics.[52-57] Among these, the Kelly-Tyson model adequately describes the mechanical behavior of discontinuous fiber reinforced composites.[57] This model assumes the interfacial shear strength, τ, of the polymer-fiber interfacial bond is constant along the length of the fiber. It defines a critical fiber aspect ratio, $(l/d)_c$, as the ratio of the fiber length to fiber diameter below which shear stress cannot be effectively transferred from the matrix to the fiber:

$$\left(\frac{l}{d}\right)_c = \frac{\sigma_f}{2\tau}$$

Equation 2-1: Critical fiber aspect ratio

σ_f is the ultimate tensile strength of the fiber. As the fiber aspect ratio exceeds the critical aspect ratio, more of the stress is transferred to the fiber and composite failure is accompanied by fiber fracture.

The fiber reinforcement efficiency is a measure of the reinforcement effectiveness of discontinuous fibers compared to their continuous, unidirectional counterpart, which represent the upper strength limit. It is formally defined as the ratio of the discontinuous and unidirectional fiber composite strengths at the same fiber composition. Poor interfacial bonding, misaligned fiber orientation and short fiber lengths will cause the fiber reinforcement efficiency to be low. Figure 2-2 shows the theoretical fiber reinforcement efficiency as a function of multiples of the critical fiber aspect ratio for an aligned, discontinuous fiber composite. The Kelly-Tyson model and rule of mixtures were used to calculate the strengths of the discontinuous and unidirectional fiber composites, respectively. Fiber reinforcement efficiency increases with increasing fiber aspect ratio because longer fibers can sustain greater stress without breakage or matrix pull-out. This behavior was confirmed using the Kelly-Tyson model to approximate the interfacial shear strength and fiber reinforcement efficiencies of injection molded short and long glass reinforced polyamide-6,6. The fiber reinforcement efficiency was indeed greater for long fiber composites compared to those with shorter fibers, while the interfacial shear strength was marginally affected.[58]

Current PAEK short fiber composites achieve a maximum fiber reinforcement efficiency of about 40% (Figure 2-2) as calculated from ultimate tensile strength data for commercially available materials.[59, 60] At five times the critical aspect ratio, it is theoretically possible to achieve
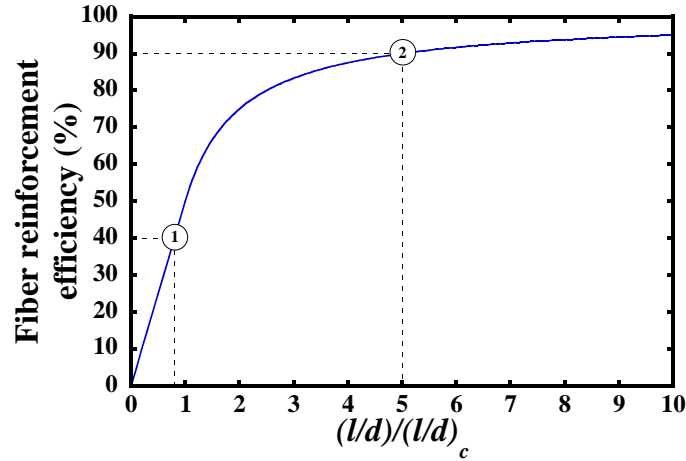
Figure 2-2: Theoretical fiber reinforcement efficiency predicted by the Kelly-Tyson model as a function of multiple of critical fiber aspect ratio$(l/d)_c$. Point 1 indicates the maximum reinforcement efficiency for current short carbon fiber reinforced PAEKs. Point 2 represents the practical target reinforcement efficiency for next generation LFT composites based on PAEKs.

90% of the mechanical properties of the unidirectional composite (Figure 2-2). This is a practical target for next generation long fiber thermoplastic composites, which can be achieved through a combination of long fibers (increased fiber aspect ratio) and improved PAEK-carbon fiber interfacial bond (decreased critical fiber aspect ratio). The typical length of carbon fibers in state of the art discontinuous composites is less than 0.5 mm, which means the average fiber length must increase to ~2.5 mm to achieve 90% of the mechanical properties of unidirectional composites without improving interfacial bonding. In reality, the fiber length may only need to be increased 2-3 fold if the interfacial shear strength of a PAEK matrix is doubled through surface modification of carbon fibers.

Figure 2-3(a) & (b) show the tensile properties of PEEK and PEKK-based short discontinuous carbon fiber composites. PEKK composite tensile properties were obtained according to ASTM D638,[60] but the same for PEEK composites reported here were obtained from Victrex datasheets[59] and were reportedly measured according to ISO 527, which produces higher values compared to ASTM D638. The overall trend demonstrates a phenomenon that is common

to all discontinuous fiber reinforced thermoplastics with fiber loadings greater than about 20 vol%. Ultimate tensile strength increases linearly as tensile modulus increases (achieved by adding up to 0.2 volume fraction carbon fiber). Tensile moduli will continue to increase linearly between 0.2 and 0.4 fiber volume fraction, while the gain in ultimate tensile strength is reduced. Finally, tensile strength plateaus at a constant value as the fiber volume fraction is increased
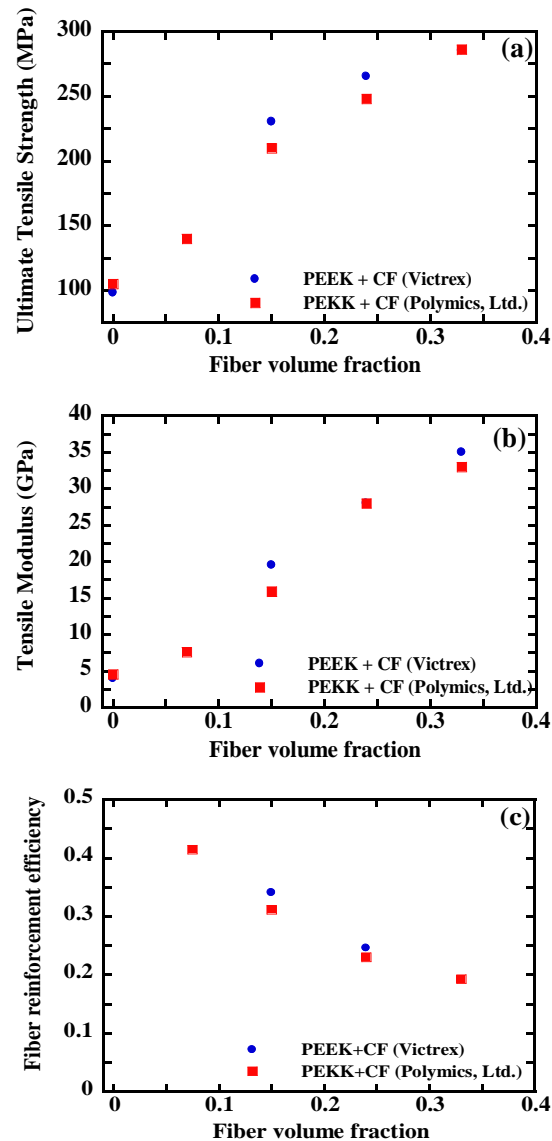
Figure 2-3: Tensile properties as a function of fiber volume fraction for PEEK and PEKK reinforced with short carbon fiber: (a) ultimate tensile strength, (b) tensile modulus and (c) fiber reinforcement efficiency.[59, 60]

above ~0.4. As Figure 2-3(c) shows, the fiber reinforcement efficiency decreases significantly with increasing fiber volume fraction. This is a major challenge currently limiting the strength performance of discontinuous carbon fiber composites.

Possibly, the large number of defects (fiber ends) in the composite at fiber loadings above 40 wt% counteract the load bearing ability of reinforcing fibers. Alternatively, the dispersion of the fibers or the fiber-to-fiber distance is inadequate to efficiently transfer load from the matrix to individual fibers. Figure 2-2 and Figure 2-3 suggest that the potential exists to significantly increase the strength of high modulus carbon fiber polymer composites by reducing defects and improving dispersion and fiber wetting. We propose that high strength, high modulus composites can be achieved by a combination of long fibers at a compositional loading below a critical value (~40 wt%) and fiber-matrix interfacial engineering.

The targeted mechanical properties for next generation LFT composites based on PAEKs are identified by the dotted region in Figure 2-1. These materials should be suitable for high volume production by injection molding yet exhibit comparable stiffness and strength to their compression molded and unidirectional carbon fiber composite counterparts. Long fibers should be used in order to achieve these target properties; however, carbon fiber length retention during melt processing is limited by the high shear stresses in PAEK polymer melts. Therefore, the critical aspect ratio must simultaneously be reduced. Based on the Kelly-Tyson model, this can be achieved by strengthening the PAEK-carbon fiber bond through interfacial engineering.

2.3 Interfacial Engineering

The neat carbon fiber surface is graphitic and relatively inert toward PAEKs, so obtaining a strong interfacial bond requires surface activation through additional chemical and/or physical treatments.[61] Typical surface treatment strategies include surface sizing, electrochemical

oxidation, plasma treatment, and grafting. Table 2-2 lists examples in which these techniques were used to improve the interfacial bond between various PAEKs and carbon fiber.

Table 2-2: Techniques used to improve the PAEK-carbon fiber interfacial bond

Fiber surface treatments	Description	Advantages	Disadvantages	References
Sizing agent	Carbon fibers are coated with a thin layer of a polymeric interfacial modifier (called sizing) before incorporation into the same or different thermoplastic matrix	Existing commercial infrastructure	Limited to physical interfacial interactions, requires VOCs	61-65
Plasma treatment	Exposure to a carefully selected plasma reaction gas (air, N_2, O_2) introduces the desired chemical functionality onto the fiber surface	Dry system (no solvents)	Over exposure damages fiber, difficult to scale-up	61, 66-69
Electrochemical oxidation	Oxygen functionality is introduced uniformly on the fiber surface by exposure to an electrochemical bath	Exposure conditions easily controllable	Over exposure damages fiber, wet system	61, 70, 71
Surface grafting	Organic and/or inorganic compounds undergo chemical reaction with the carbon fiber surface in order to improve interfacial transport properties and bonding with polymer matrices	Many possibilities for chemical and physical interfacial interactions	Relatively difficult and costly due to multi-step processes	72-74

2.3.1 Sizing

Sizings are low molecular weight or fully developed polymers that are applied directly to the carbon fiber surface to enhance matrix polymer adhesion and to reduce fiber damage during fiber processing. Carbon fiber sizing chemistries based on urethane and epoxy thermosets are well-known and readily available,[75-77] but are not compatible with PAEKs nor are they stable at higher service temperatures. Such thermoset-based sizing chemistries are suitable for most thermoset matrices because they form covalent linkages with both the matrix and carbon fiber

surface. They are not compatible with PAEK thermoplastics due to the low chemical reactivity of the main polymer chain. Compatible sizings that improve the interaction between carbon fiber and PAEK thermoplastic matrices typically function by entangling chains with the matrix rather than chemical linkages; thus, some degree of mixing between the sizing compound and the PAEK matrix is required.

Polyether imide (PEI) is a good candidate sizing material for carbon fiber in PEEK-based composites because it is thermally stable and exhibits at least partial solubility with polyether ether ketone.[78-80] Giraud et al. obtained a continuous interface between carbon fibers and PEEK matrix using PEI dispersions prepared by an emulsion/evaporation technique.[62] Figure 2-4 shows the difference between the interfaces of unsized and PEI-sized carbon fiber PEEK composites. The PEI-sized fibers exhibit a continuous interface with the PEEK matrix, suggesting improved adhesion to the PEI sized carbon fibers. Similarly, PEKK-sized carbon fibers exhibit a continuous interface with a PEEK matrix, while epoxy-sized fibers do not.[81] The same study demonstrates that the PEKK-sized fiber composite is not affected by kerosene saturation due to the solvent resistance of polyketones.

Sizing agents with chemical motifs similar to the polymer matrix have been effective in improving adhesion to the carbon fiber surface, such as a PPEK/carbon fiber composite with PPEK-sized carbon fibers.[82] This resulted in improved wettability of the carbon fiber surface and a 30% improvement in apparent interfacial shear strength compared to unsized carbon fibers.[64]

Sizing application is historically the common way to improve fiber-matrix interaction while simultaneously facilitating the handling of fiber tows. Many carbon fiber manufacturers
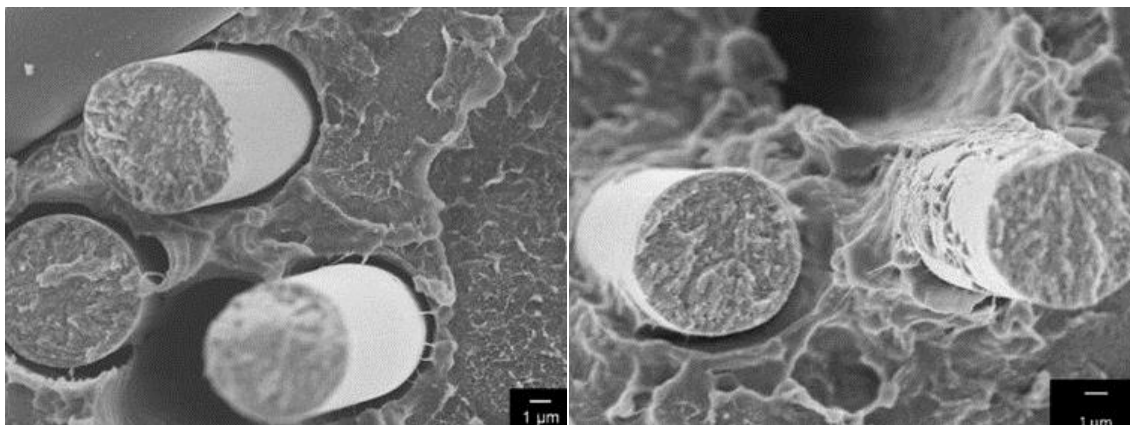
Figure 2-4: PEEK/carbon fiber composite containing (left) unsized carbon fibers and (right) PEI-sized carbon fibers.[62] Reprinted from Applied Surface Science, Copyright 2013, with permission from Elsevier.

already have the equipment and infrastructure required to produce sized carbon fibers on a commercial scale. Furthermore, sizings will continue to play a major role in fiber surface modification. Unfortunately, there are few commercially available sizings that are compatible with PAEK matrices. In fact, these composites usually contain unsized fibers that have been electrochemically or plasma treated. Sizing chemistries based on amorphous and semi-crystalline PAEKs are necessary to improve the service lifetime and maximum allowable operating temperature of PAEK composites.

2.3.2 Plasma Treatment

Plasma treatment involves exposure of the carbon fiber to a plasma gas to increase surface roughness and introduce polar functional groups to the carbon fiber surface in order to improve wettability and adhesion of the PAEK matrix.[83-85] This is achieved using a variety of gases, such as air, oxygen, ammonia and nitrogen. Oxygen plasma treatment increases fiber surface acidity and hydrophobicity through the addition of carbonyl, carboxylic acid and alcohol residues.[84-86] Other applications of plasma treatment on fibers and textiles are described elsewhere.[87, 88]
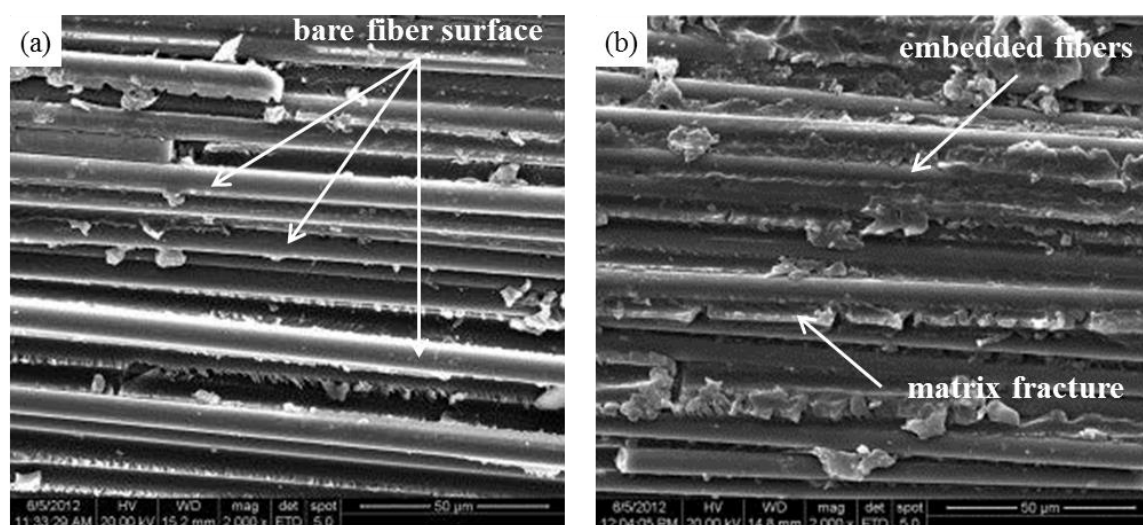
Figure 2-5: SEM images of fracture surfaces for PAEK composites containing (a) untreated and (b) oxygen plasma treated carbon fibers.[67] Reprinted from Polymer Composites, Copyright 2013, with permission from Wiley.

Li et al. achieved approximately a 12% improvement in the interlaminar shear strength of a PAEK-carbon fiber system by using oxygen plasma treated carbon fibers.[67] They found that the surface roughness and oxygen surface composition increases with increasing amounts of oxygen plasma treatment. Characterization was done through X-ray photoelectron spectroscopy (XPS), a surface characterization technique commonly used to characterize the surface chemistry of carbon fiber and polymers and their interactions at buried interfaces.[89, 90] Figure 2-5 shows the differences in the fracture morphologies of untreated and oxygen plasma treated PAEK-carbon fiber interlaminar shear stress specimens. The PAEK matrix exhibited poor adhesion to untreated carbon fibers (Figure 2-5(a)), resulting in mechanical failure at the interface due to matrix debonding. The same matrix showed enhanced adhesion to plasma treated carbon fibers resulting in fracture of the matrix, while leaving the interface significantly more intact (Figure 2-5(b)). They also found that excessive oxygen plasma treatment results in reduced interlaminar shear strength and reduced composite performance. In another example, Xie et al. found that plasma modified carbon fibers in a polyimide matrix have 20% greater interfacial shear strength

compared to unmodified fibers when exposed for 32 s, but the increase was only 5% when exposed for 64 s.[91]   They also found that single fiber tensile strength may decrease with prolonged plasma exposure.

A 13% improvement in interlaminar shear strength was reported for a PPESK-carbon fiber system using oxygen plasma treated carbon fibers.[66] They similarly found that the failure mode for plasma-treated carbon fibers is different from untreated composites and that there is an optimum plasma treatment time beyond which the carbon fiber becomes damaged from prolonged exposure. Residual polymer remains on the fiber surface after exposure to concentrated sulfuric acid, suggesting that interfacial bonds may be covalent. FT-IR spectoscopy indicates the presence of ketene residues, which are not present in the neat polymers.

Abrasive wear studies were conducted on composites of PEEK and carbon fabric exposed to cold remote nitrogen oxygen plasma treatment.[68, 69, 92] The composite tensile strength of treated specimens improved 8% compared to untreated composites, suggesting an increase in interfacial shear strength. A more recent study from the same research group shows the plasma modifications result in a 22% increase in interfacial shear strength and a 26% increase in wear resistance despite a 5% reduction in single fiber tensile strength.[93]

Overall, plasma surface treatment has been succesful in achieving improvements in interfacial bonding and shear strength, but over-exposure to plasma can reduce the tensile strength of individual fibers. Thus, successful plasma modification requires tight control of optimal exposure conditions to produce an improved interface without sacrificing fiber mechanical properties. Plasma surface modifications will likely play a minor role in next-generation composites because the improvements to composite properties are only marginally better than the improvements obtained from currently widespread electrolytical treatments of carbon fibers.

2.3.3 Electrochemical Oxidation

Electrochemical oxidation is used to introduce polar functionalities to the surface of carbon fibers which in turn improves the interfacial interaction between fiber and polymers. Electrochemical oxidation is currently the industry standard for increasing surface activity of carbon fiber and is performed as the final step in its manfacture. Types of functional groups added to the carbon fiber surface include hydroxyl (C-OH), carbonyl (C=O) and carboxyl (COOH).[94-97] Liu et al. studied the effect of electrolytic oxidation in aqueous ammonium oxoalate solutions on the surface properties of PAN-based carbon fibers.[98] They found that fine control of the oxidation treatment parameters not only introduced active surface functional groups, but also removed weak carbonaceous components from the surface thereby exposing a more crystalline graphitic surface. This improved the interfacial shear stength with an epoxy matrix by nearly 10% and increased the fiber tensile strength by 16%. In a similar study, carbon fibers electrochemically oxidized in aqueous ammonium bicarbonate solution showed a 40% improvement of interfacial shear strength in an epoxy matrix, while preserving carbon fiber mechanical strength.[99] Figure 2-6 compares the fracture morphologies of micro-bond test specimens containing untreated and electrochemically oxidized carbon fibers. After micro-bond tests, the untreated carbon fiber has little to no residual epoxy resin bonded to the surface, while the oxidized carbon fiber has a significant amount of residual epoxy resin. Similar interfacial bonding characteristics have been observed in composites based on PAEK matrices as discussed below.

Carbon fibers are pretreated with piranha (sulfuric acid and hydrogen peroxide) and chromate solutions to oxidize the surface and promote bonding with PEEK matrices.[100] XPS indicates an increase in surface O/C ratio accompanied by an increase in surface hydroxyl and carboxyl groups. The composites with chromate-treated fibers increased in interlaminar shear
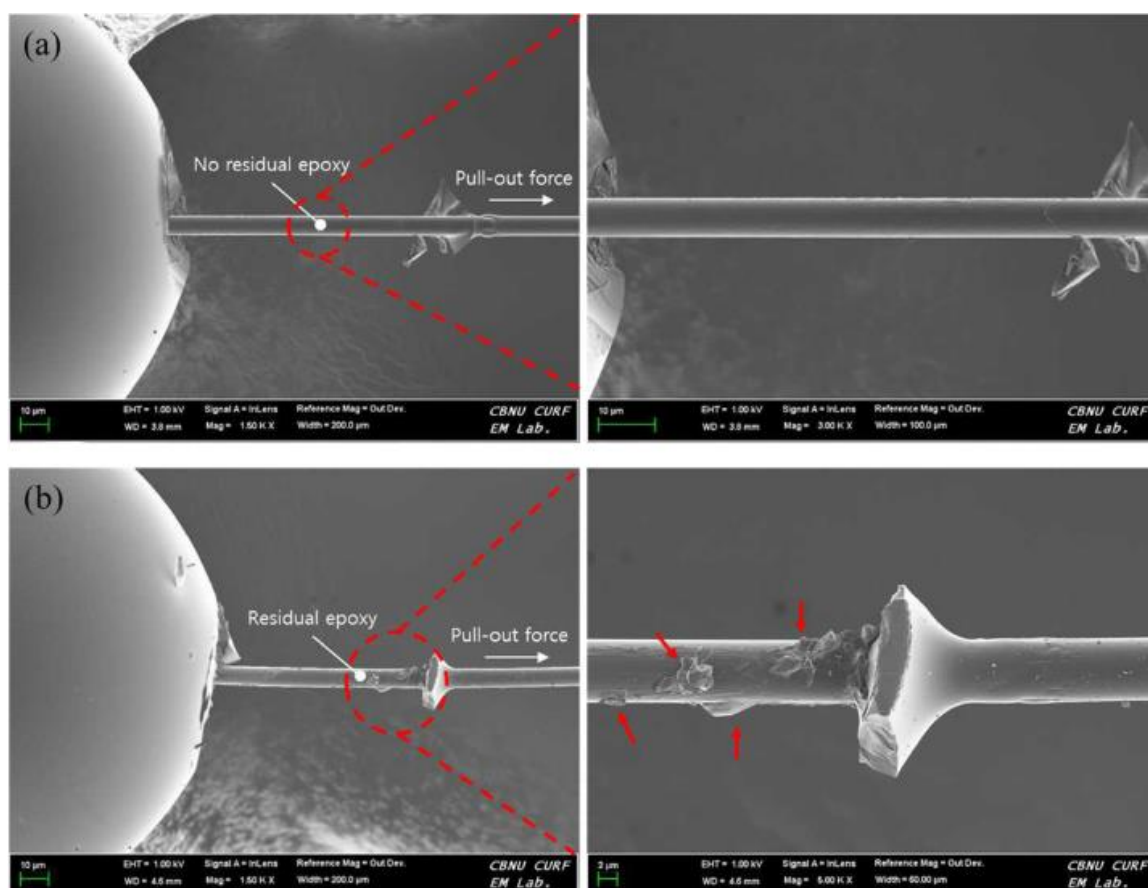
Figure 2-6: SEM images of epoxy/carbon fiber micro-bond test specimens after fracture containing (a) untreated and (b) electrochemically oxidized carbon fibers.[99] Reprinted from Carbon Letters, Copyright 2016, with permission from Korean Carbon Society.

strength by 25%, while the carbon fibers treated in a piranha solution at 100 °C showed a 14% increase in interlaminar shear strength. Fractured composite specimens containing untreated fibers and fibers treated at room temperature with piranha solutions exhibit clear debonding of the fibers and the matrix, which correlates with the marginal increase in interlaminar shear strength. In contrast, composites where carbon fibers are treated with piranha or chromate solutions at 100 °C have an intact interface after fracture, suggesting strong adhesion with the PEEK matrix.

An example of the use of electrochemically oxidized carbon fibers in PEKK matrices was reported by Sherwood et al., where surface interactions between PEKK and electrochemicallly oxidized pitch-based carbon fibers were investigated using XPS.[70] They did not find any evidence

to suggest that PEKK reacts with untreated carbon fibers. On the other hand, chemistry between PEKK and treated carbon fibers appears to occur. Electrochemical oxidation in nitric acid increases the total amount of oxidized surface carbon and produces hydrogen-bridged oxide structures, carbonyl, and carboxyl groups on the surface of the carbon fiber, while decrasing the amount of graphitic carbon. Chemical reactions were proposed between PEKK carbonyl groups and hydrogen-bridged oxide structures on the carbon fiber surface. The authors also found evidence that these interfacial interactions are susceptible to degradation upon exposure in saline solution at 92°C for 10 days. The authors did not report any effect of the electrochemical oxidation on the mechanical performance.

Electrochemical oxidation to enhance the chemical reactivity of the carbon fiber surface significantly improves the interfacial bond in composites. In addition to relying on direct interaction with PAEK matrices, the potential exists for further functionalization of the carbon fiber surface via oligomer grafting techniques that can further improve the interfacial bond.

2.3.4 Surface Grafting

Surface grafting relies on a direct chemical reaction with the carbon fiber surface resulting in a covalent bond between surface functional groups and the polymer and/or interfacial modifier. There are limited examples of surface grafting of carbon fibers for thermoplastic compatability, and even fewer relating to PAEKs. Soulis et al. reported electrochemical grafting of 4-phenoxybenzoic acid onto oxidized carbon fibers to improve wetability by PAEKs, such as PEK and PEEK.[73] In this work, carbon fibers were electrochemically oxidized in sulfuric acid in order to provide surface reactivity for electrochemical grafting of 4-phenoxybenzoic acid (4-PBA). The 4-PBA coating improves the thermal degradation resistance of electrochemically treated carbon fiber. They did not report any effects on the wettability of carbon fiber by PAEK
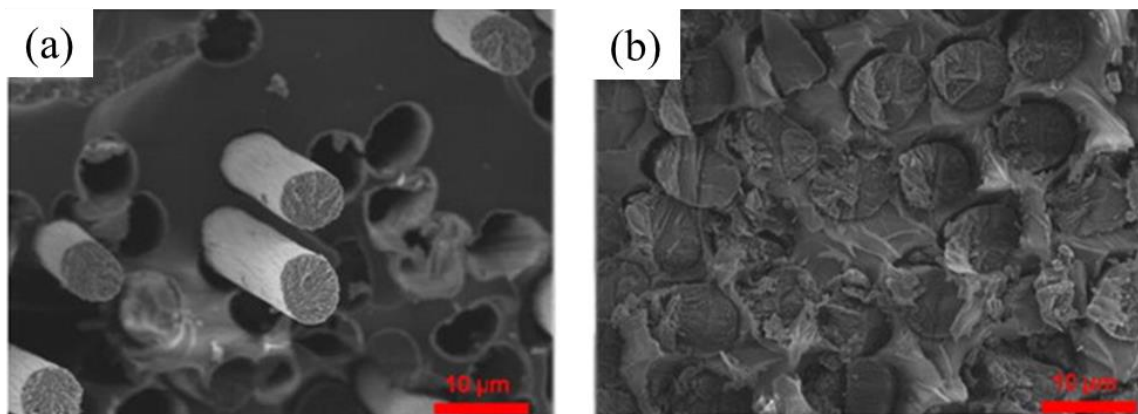
Figure 2-7: SEM images of fracture surface of epoxy composite containing (a) untreated and (b) CNT surface grafted carbon fibers.[101] Reprinted from Materials Letters, Copyright 2014, with permission from Elsevier.

or mechanical performance.

There are examples of grafting nanoparticles to the surface of carbon fiber in order to improve matrix bonding.[72] Zhang et al. reported carbon nanotube/carbon fiber multi-scale reinforcement prepared by grafting multiwalled carbon nanotubes onto the surface of carbon fibers.[74] Similarly, a step-wise reduction technique to functionalize carbon fibers with multiwall carbon nanotubes results in a two-fold improvement in interfacial bonding with an epoxy matrix.[101] The fracture morphologies of epoxy composites with untreated and CNT surface grafted carbon fibers is shown in Figure 2-7. Untreated fibers cleanly pull-out from the matrix, while fibers with CNTs grafted onto their surface break at the fracture face without matrix pull-out. Intermediate NH_2-functionalized carbon fibers also exhibit a 75% improvement in interfacial bonding with the same epoxy matrix. This suggests that mechanical interlocking of chains is more effective than covalent linkages at the fiber-epoxy matrix. Li et al. obtained similar results using a polyamidoamine to form a carbon nanotube heirarchical structure.[102] We expect that this mechanism for enhancing interfacial bonding can be adapted to PAEK matrices because it

appears to not depend on specific interactions or chemistries; instead, it relies only on fiber surface area. A more in-depth discussion of hierarchical composites based on carbon nanotubes can be found elsewhere.[103]

Although there are not many examples of the use of surface-grafted carbon fibers in PAEK matrices, their performance in other thermoplastic and thermosets suggests promising opportunities for PAEK composites. Surface grafting will be essential to pushing the limits on interfacial shear strength in PAEK matrices because it creates either covalent linkages between the polymer and the fiber or significantly increases the fiber surface area without sacrificing mechanical properties.

2.4 Roadmap for Next Generation Carbon Fiber Composites

The next generation of discontinuous fiber PAEK composites must exhibit exceptional strength and stiffness (comparable to unidirectional fiber composites), operate at elevated temperatures, and be suitable for high volume manufacturing techniques. The target tensile properties identified in Figure 2-1 will be achieved in part through the continued use of discontinuous fibers sufficiently longer than the critical fiber length. In addition, improvements in the interfacial fiber-matrix bond strength will reduce the critical fiber length, making fiber retention during high shear molding processes less critical.

Interfacial engineering is the key to strengthening the fiber-matrix bond, either through fiber sizing, plasma treatment, electrochemical oxidation and/or surface grafting. Advances in carbon fiber plasma treatment techniques have allowed for modest increases in the interfacial bond strength, while the surface chemistries are confined to the limited choice of plasma gases. Electrochemical oxidation is the current industry standard and offers similar functionalization of the carbon fiber surface. Unfortunately, most commercial electrolytic oxidation processes are not

optimized to modify carbon fibers for compatibility with PAEKs, rather they are intended to prepare the surface of the fibers for improved bonding with thermoset matrices.

Application of a compatible sizing agent to the fiber surface is the simplest interfacial modification technique, but few sizing chemistries are currently available and compatible with high temperature PAEKs. Developments in this area would have short-term commercial viability because the manufacturing infrastructure for sizing application is already established. Nevertheless, we expect improvements in mechanical properties of sized fiber composites will be marginal compared to grafted fiber composites because the former is based on relatively weak physical interactions while the latter utilizes strong covalent bonds. Surface grafting of carbon fibers is the least investigated interfacial modification technique to date, but, it has the potential to drastically improve the mechanical performance of PAEK carbon fiber reinforced composites.

Surface modification chemistries can be adapted from available crosslinking chemistries for PAEKs. Both sizing and grafting methods to improve the interfacial bond have the benefit of being tailorable to specific PAEK molecular architectures. Short-term enhancements in the mechanical properties of PAEK carbon fiber composites will likely be achieved through new sizing chemistries that can be coated onto fibers using existing industrial equipment. We predict that long-term improvements toward the next generation of long carbon fiber composites that push the limits of polymer mechanics will rely on the use of surface grafting techniques and chemistries tailored to PAEK matrices.

2.5 References

1.   Srivastava, R. B., Upreti, M. C., Awasthi, M. and Mathur, G. N. *Indian Journal of Engineering and Materials Sciences* **2003**, *2*, 143-147.

2.   Iannone, M., Esposito, F. and Cammarano, A. In AIP Conference Proceedings,Proceedings of the 7th International Conference on Times of Polymers and Composites (TOP), Ischia, Italy, Jun 22-26, 2014; Amer Inst Physics: Melville, 2014.

3.   Diez-Pascual, A. M., Naffakh, M., Marco, C., Ellis, G. and Gomez-Fatou, M. A. *Progress in Materials Science* **2012**, *7*, 1106-1190.

4.   Ng, S. J. and Meilunas, R. J. *Sampe Journal* **2007**, *6*, 17-20.

5.   Cohen, D. *Composites Part a-Applied Science and Manufacturing* **1997**, *12*, 1035-1047.

6.   Migliaresi, C., Nicoli, F., Rossi, S. and Pegoretti, A. *Composites Science and Technology* **2004**, *6*, 873-883.

7.   Vaidya, U. K., Chawa, K. K., Thattaiparthasarthy, K. B. and Goel, A. *JOM* **2008**, *4*, 43-49.

8.   Saha, P., Chowdhury, S., Roy, D., Adhikari, B., Kim, J. K. and Thomas, S. *Polymer Bulletin* **2016**, *2*, 587-620.

9.   Hamdi, S. E., Delisee, C., Malvestio, J., Da Silva, N., Le Duc, A. and Beaugrand, J. *Composites Part a-Applied Science and Manufacturing* **2015**, 1-9.

10.   Yao, J., Jin, J. H., Lepore, E., Pugno, N. M., Bastiaansen, C. W. M. and Peijs, T. *Macromolecular Materials and Engineering* **2015**, *12*, 1238-1245.

11.   Cai, P., Li, Z. L., Wang, T. M. and Wang, Q. H. *Tribology International* **2015**, 109-116.

12.   Unterweger, C., Bruggemann, O. and Furst, C. *Polymer Composites* **2014**, *2*, 227-236.

13.   Lyu, W. Y., Cui, Y. H., Zhang, X. J., Yuan, J. Y. and Zhang, W. *Journal of Applied Polymer Science* **2016**, *24*, 9.

14.   Rahate, A. S., Nemade, K. R. and Waghuley, S. A. *Reviews in Chemical Engineering* **2013**, *6*, 471-489.

15.   Kim, J. H., Kawai, M., Yonezawa, S. and Takashima, M. *Journal of Fluorine Chemistry* **2008**, *7*, 654-657.

16.   Odochian, L., Moldoveanu, C., Mocanu, A. M. and Carja, G. *Thermochimica Acta* **2011**, *1-2*, 205-212.

17.   Guo, Z. H., Lin, P. J., Xu, Q. Y., Shao, Q., Wang, Y. P., Qiu, G. and Wang, Y. M. *Applied Mechanics and Materials* **2013**, 138-142.

18.   Teng, H. X. *Applied Sciences-Basel* **2012**, *2*, 496-512.

19.   Gan, D. J., Lu, S. Q., Song, C. S. and Wang, Z. J. *Macromolecular Materials and Engineering* **2001**, *5*, 296-301.

20.   Yan, T., Chen, M. F., Xu, Q. and Cai, M. Z. *Journal of Polymer Research* **2013**, *1*,

21. Patel, P., Hull, T. R. and Moffatt, C. *Fire and Materials* **2012**, *3*, 185-201.

22. Mazur, R. L., Oliveira, P. C., Rezende, M. C. and Botelho, E. C. *Journal of Reinforced Plastics and Composites* **2014**, *8*, 749-757.

23. McLauchlin, A. R., Ghita, O. R. and Savage, L. *Journal of Materials Processing Technology* **2014**, *1*, 75-80.

24. Hamdan, S. and Swallowe, G. M. *Journal of Polymer Science Part B-Polymer Physics* **1996**, *4*, 699-705.

25. Qian, J. P., Zhou, W. X., Yu, Y. K. and Cai, M. Z. *Polymer Engineering and Science* **2013**, *11*, 2353-2359.

26. Rueda, D. R., Gutierrez, M. C. G., Ania, F., Zolotukhin, M. G. and Calleja, F. J. B. *Macromolecules* **1998**, *23*, 8201-8208.

27. Berard, N., Paventi, M., Chan, K. P. and Hay, A. S. *Macromolecular Symposia* **1994**, 379-388.

28. Meng, Y. Z., Hlil, A. R. and Hay, A. S. *Journal of Polymer Science Part A-Polymer Chemistry* **1999**, *12*, 1781-1788.

29. Meng, Y. Z., Hay, A. S., Jian, X. G. and Tjong, S. C. *Journal of Applied Polymer Science* **1997**, *8*, 1425-1432.

30. Hay, A. S., Jian, X. G. and Wang, Y.-F. U.S. Patent Application Number 12/680,510, July 7, 2011.

31. Wang, Y.-F., Hsu, T. and Hay, A. S. U.S. Patent

32. Jian, X. G., Chen, P., Liao, G. X., Zhu, X. L., Zhang, S. H. and Wang, J. Y. *Acta Polymerica Sinica* **2003**, *4*, 469-475.

33. Liu, Y. J., Jian, X. G., Liu, S. J., Zhang, J. and Wang, Z. Y. *Acta Polymerica Sinica* **1999**, *1*, 37-41.

34. Hou, M. and de Weger, D. In New Materials, Applications and Processes, Pts 1-3; J. M. Zeng, Y. H. Kim and Y. F. Chen, Eds.; **2012**; Vol. 399-401, pp 289-293.

35. McCool, R., Murphy, A., Wilson, R., Jiang, Z., Price, M., Butterfield, J. and Hornsby, P. *Proceedings of the Institution of Mechanical Engineers Part L-Journal of Materials-Design and Applications* **2012**, *L2*, 91-102.

36. Sun, C. T., Chung, I. and Chang, I. Y. *Composites Science and Technology* **1992**, *4*, 339-345.

37. Whitworth, H. A., Llorente, S. G. and Croman, R. B. *Static and dynamic performance of notched LDT PEKK composites*, 1993.

38. Pratte, J. F., Krueger, W. H. and Chang, I. Y. *Tomorrows Materials : Today, Book 1 and 2: 34th International Sampe Symposium and Exhibition* **1989**, 2229-2242.

39. Phelps, J. H., El-Rahman, A. I. A., Kunc, V. and Tucker, C. L. *Composites Part a-Applied Science and Manufacturing* **2013**, 11-21.

40. Durin, A., De Micheli, P., Ville, J., Inceoglu, F., Valette, R. and Vergnes, B. *Composites Part a-Applied Science and Manufacturing* **2013**, 47-56.

41. Rohde, M., Ebel, A., Wolff-Fabris, F. and Altstadt, V. *International Polymer Processing* **2011**, *3*, 292-303.

42. Inoue, A., Morita, K., Tanaka, T., Arao, Y. and Sawada, Y. *Journal of Composite Materials* **2015**, *1*, 75-84.

43. Ortman, K., Baird, D., Wapperom, P. and Aning, A. *Polymer Composites* **2012**, *8*, 1360-1367.

44. Luo, H. L., Xiong, G. Y., Ma, C. Y., Li, D. Y. and Wan, Y. Z. *Materials & Design* **2014**, 294-300.

45. Kim, N., Kim, D. Y., Kim, Y. J. and Jeong, K. U. *Journal of Materials Science* **2014**, *18*, 6333-6342.

46. Thomason, J. L. *Composites Part a-Applied Science and Manufacturing* **2009**, *2*, 114-124.

47. KetaSpire PEEK Design & Processing Guide. Solvay Specialty Polymers. Version 2.1, March 2016.

48. Victrex PEEK 450G test data sheet. Victrex High Performance Polymers. July 2014.

49. Vestakeep 5000G product information sheet. Evonik Industries. October 2011.

50. Li, R. S., Wu, T., Zeng, L. X., Xu, J. J. and Liu, P. Q. *Journal of Applied Polymer Science* **2014**, *16*, 9.

51. Manolakis, I., Cross, P., Ward, S. and Colquhoun, H. M. *Journal of Materials Chemistry* **2012**, *38*, 20458-20464.

52. Sarasua, J. R., Remiro, P. M. and Pouyet, J. *Journal of Materials Science* **1995**, *13*, 3501-3508.

53. Cox, H. L. *British Journal of Applied Physics* **1952**, *MAR*, 72-79.

54. Thomason, J. L. and Vlug, M. A. *Composites Part a-Applied Science and Manufacturing* **1996**, *6*, 477-484.

55. Nguyen, B. N., Kunc, V., Jin, X., Tucker, C. L. and Costa, F. *Proceedings of the American Society for Composites* **2013**,

56. Rezaei, F., Yunus, R. and Ibrahim, N. A. *Materials & Design* **2009**, *2*, 260-263.

57. Kelly, A. and Tyson, W. R. *Journal of the Mechanics and Physics of Solids* **1965**, *6*, 329-350.

58. Hassan, A., Yahya, R., Rafiq, M. I. M., Hussin, A., Sheikh, M. R. K. and Hornsby, P. R. *Journal of Reinforced Plastics and Composites* **2011**, *14*, 1233-1242.

59. Victrex, Victrex PEEK 450CA10, 450CA20, 450CA30, 450CA40 technical data sheets. www.victrex.com/en/datasheets (2014).

60. Polymics Arylmax K7522 carbon fiber filled, material test report, 2014.

61. Sharma, M., Gao, S. L., Mader, E., Sharma, H., Wei, L. Y. and Bijwe, J. *Composites Science and Technology* **2014**, 35-50.

62. Giraud, I., Franceschi-Messant, S., Perez, E., Lacabanne, C. and Dantras, E. *Applied Surface Science* **2013**, 94-99.

63. Dilsiz, N. and Wightman, J. P. *Carbon* **1999**, *7*, 1105-1114.

64. Liu, W. B., Zhang, S., Hao, L. F., Jiao, W. C., Yang, F., Li, X. F. and Wang, R. G. *Journal of Applied Polymer Science* **2013**, *6*, 3702-3709.

65. Zhang, S., Liu, W. B., Hao, L. F., Jiao, W. C., Yang, F. and Wang, R. G. *Composites Science and Technology* **2013**, 120-125.

66. Lu, C., Chen, P., Yu, Q., Ding, Z. F., Lin, Z. W. and Li, W. *Journal of Applied Polymer Science* **2007**, *3*, 1733-1741.

67. Li, W., Yao, S. Y., Ma, K. M. and Chen, P. *Polymer Composites* **2013**, *3*, 368-375.

68. Sharma, M., Bijwe, J. and Mitschang, P. *Tribology International* **2011**, *2*, 81-91.

69. Tiwari, S., Sharma, M., Panier, S., Mutel, B., Mitschang, P. and Bijwe, J. *Journal of Materials Science* **2011**, *4*, 964-974.

70. Wang, Y. Q., Zhang, F. Q. and Sherwood, P. M. A. *Chemistry of Materials* **2001**, *3*, 832-841.

71. Pittman, C. U., Jiang, W., Yue, Z. R., Gardner, S., Wang, L., Toghiani, H. and Leon, C. *Carbon* **1999**, *11*, 1797-1807.

72. Shiba, K., Tagaya, M., Samitsu, S. and Motozuka, S. *ChemPlusChem* **2014**, *2*, 197-210.

73. Soulis, S., Triantou, D. and Simitzis, J. *Journal of Applied Polymer Science* **2013**, *3*, 1466-1478.

74. He, X., Zhang, F., Wang, R. and Liu, W. *Carbon* **2007**, *13*, 2559-2563.

75. Zhang, Q. B., Liu, L., Jiang, D. W., Yan, X. R., Huang, Y. D. and Guo, Z. H. *Journal of Composite Materials* **2015**, *23*, 2877-2886.

76.   Ge, H. Y., Ma, X. L. and Liu, H. S. *Journal of Applied Polymer Science* **2015**, *16*, 9.

77.   Liu, Z. Q., Tian, Y. H., Kang, S. M. and Zhang, X. J. *Journal of Applied Polymer Science* **2012**, *5*, 3490-3499.

78.   Hsiao, B. S. and Sauer, B. B. *Journal of Polymer Science Part B-Polymer Physics* **1993**, *8*, 901-915.

79.   Crevecoeur, G. and Groeninckx, G. *Macromolecules* **1991**, *5*, 1190-1195.

80.   Shibata, M., Fang, Z. J. and Yosomiya, R. *Journal of Applied Polymer Science* **2001**, *5*, 769-775.

81.   Giraud, I., Franceschi, S., Perez, E., Lacabanne, C. and Dantras, E. *Journal of Applied Polymer Science* **2015**, *38*, 5.

82.   Liu, W. B., Zhang, S., Hao, L. F., Jiao, W. C., Yang, F., Li, X. F. and Wang, R. G. *Polymer Composites* **2013**, *11*, 1921-1926.

83.   Li, R. Z., Ye, L. and Mai, Y. W. *Composites Part a-Applied Science and Manufacturing* **1997**, *1*, 73-86.

84.   Bubert, H., Ai, X., Haiber, S., Heintze, M., Bruser, V., Pasch, E., Brandl, W. and Marginean, G. *Spectrochimica Acta Part B-Atomic Spectroscopy* **2002**, *10*, 1601-1610.

85.   Wu, G. M. *Materials Chemistry and Physics* **2004**, *1*, 81-87.

86.   Bismarck, A., Kumru, M. E. and Springer, J. *Journal of Colloid and Interface Science* **1999**, *1*, 60-72.

87.   Abd Jelil, R. *Journal of Materials Science* **2015**, *18*, 5913-5943.

88.   Zille, A., Oliveira, F. R. and Souto, A. P. *Plasma Processes and Polymers* **2015**, *2*, 98-131.

89.   Sherwood, P. M. A. *Journal of Electron Spectroscopy and Related Phenomena* **1996**, *3*, 319-342.

90.   Weitzsacker, C. L., Xie, M. and Drzal, L. T. *Surface and Interface Analysis* **1997**, *2*, 53-63.

91.   Xie, J. F., Xin, D. W., Cao, H. Y., Wang, C. T., Zhao, Y., Yao, L., Ji, F. and Qiu, Y. P. *Surface & Coatings Technology* **2011**, *2-3*, 191-201.

92.   Sharma, M., Bijwe, J. and Mitschang, P. *Wear* **2011**, *9–10*, 2261-2268.

93.   Sharma, M., Bijwe, J., Mader, E. and Kunze, K. *Wear* **2013**, *1-2*, 735-739.

94.   Gardner, S. D., Singamsetty, C. S. K., Booth, G. L., He, G. R. and Pittman, C. U. *Carbon* **1995**, *5*, 587-595.

95. Yue, Z. R., Jiang, W., Wang, L., Gardner, S. D. and Pittman, C. U. *Carbon* **1999**, *11*, 1785-1796.

96. Guo, Y. X., Liu, J. and Liang, J. Y. *Journal of Materials Science & Technology* **2005**, *3*, 371-375.

97. Guo, Y. X., Liu, J. and Liang, J. Y. *Journal of Inorganic Materials* **2009**, *4*, 853-858.

98. Liu, J., Tian, Y., Chen, Y., Liang, J., Zhang, L. and Fong, H. *Materials Chemistry and Physics* **2010**, *2-3*, 548-555.

99. Kim, D., An, K., Bang, Y., Kwac, L., Oh, S. and Kim, B. *Carbon Letters* **2016**, *1*, 32-39.

100. Yapici, U., Pan, L., Xu, F. and Cao, J. M. *Advanced Materials, Mechanics and Industrial Engineering* **2014**, 66-72.

101. Liu, Y. T., Wu, G. P. and Lu, C. X. *Materials Letters* **2014**, 75-79.

102. Peng, Q., He, X., Li, Y., Wang, C., Wang, R., Hu, P., Yan, Y. and Sritharan, T. *Journal of Materials Chemistry* **2012**, *13*, 5928-5931.

103. Qian, H., Greenhalgh, E. S., Shaffer, M. S. P. and Bismarck, A. *Journal of Materials Chemistry* **2010**, *23*, 4751-4762.

Chapter 3

**Enhancing Resistance of PEKKs to High Temperature Steam
Through Crosslinking and Crystallization Control**

3.1 Introduction

Poly(aryl ether ketone)s (PAEKs) are a family of high performance thermoplastics which offer excellent chemical and thermal resistance, good mechanical properties and manufacturability into end-use components for critical applications. They find widespread use in the medical,[1-3] semiconductor manufacturing,[4, 5] aerospace,[6-10] automotive[11, 12] and petrochemical[13, 14] industries. Poly(ether ether ketone) (PEEK) (Figure 3-1(a)) is the most widely available of the PAEK family, has the largest production volume, and performs well in most sealing and connector applications that involve contact with drilling fluids and sour (sulfur-containing) crude oil under high pressure and high temperature conditions.
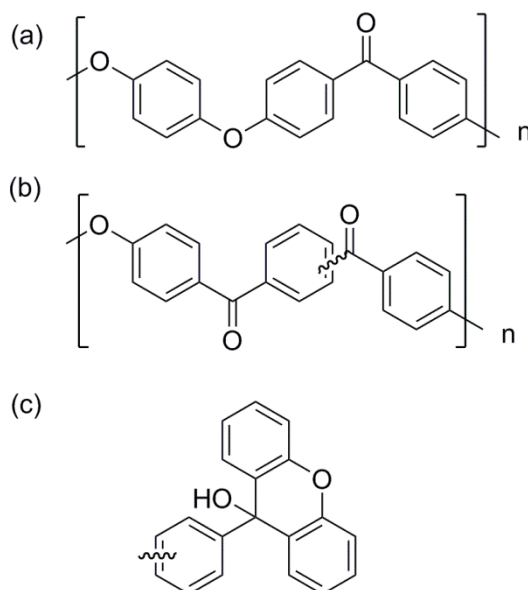
Figure 3-1: Chemical structure of (a) PEEK, (b) PEKK(T/I) and (b) 9-phenylenexanthydrol crosslink precursor.

Despite its superior performance in many downhole applications, PEEK is not suitable for the highest temperature steam injection strategies utilizing cyclic steam stimulation,[15] steam flooding[16] and steam assisted gravity drainage,[17] for recovery of heavy oils from oil sand formations. Steam injection conditions can be as extreme as ~2200 psi and ~350°C in order to heat heavy oil and reduce its viscosity, thereby facilitating recovery. Even with carbon and glass fiber reinforcement, PEEK does not sufficiently retain mechanical properties at these conditions because it is very near its melting point. Handling and containment of high pressure, high temperature steam requires a thermally stable, highly creep resistant material that can provide an effective seal for longer service periods. Other requirements include resistance to high temperature steam, appropriate balance of creep resistance and ductility at service temperature and facile melt processability and machinability into end-user components.

Looking to other members of the PAEK family, there are other candidate materials with higher melting temperatures and similar chemical resistance and mechanical properties. Many of the polymer chemistries currently available, along with thermal and mechanical properties, are discussed in a recent review of next generation of carbon fiber reinforced PAEKs.[18] Melting and glass transition temperatures of PAEKs increase monotonically as the keto/ether ratio increases.[19] In addition, higher degree of crystallinity and creep resistance are generally achievable through higher keto/ether ratios. For example, PEK (50% keto) and PEKEKK (60% keto) offer improved creep resistance compared to PEEK and are commercially available, though they are considerably more expensive and are easily susceptible to degradation and gelation due to their high processing temperature. PEKK (66% keto) is a more viable candidate for high temperature steam applications, because it has the highest melting and glass transition temperatures among the PAEK family, exhibits a balance of creep resistance and ductility, and is readily available to manufacturers and engineers.

PEKK is synthesized through Friedel-Crafts acylation of biphenyl ether and a mixture of terephthaloyl and isophthaloyl chlorides in a suitable organic solvent with aluminum chloride catalyst. While it has the highest keto/ether ratio of any commercially available PAEK, its crystallinity and thermomechanical behavior can be tuned by controlling the monomer stereochemistry. The ratio of tere and iso phthaloyl monomers (referred to as T/I ratio) in the polymerization reaction effects stiffness and mobility of the resulting polymer chain, thereby control of thermal and mechanical properties is achievable.[20] PEKK with a higher T/I ratio exhibits high crystallinity, higher temperature thermal transitions and superior creep resistance, while PEKK with a lower T/I ratio exhibits reduced crystallinity, lower temperature thermal transitions and good ductility. This tunability allows PEKK to find uses in wide-ranging applications that require very different enabling thermal and mechanical characteristics.

Little has been reported on the effect of high temperature steam on PAEKs, however. A series of high temperature steam treatment studies of PEEK, PEKK and their blends with poly(benzimidazole) revealed that moisture absorption by these materials is reversible when exposed to steam up to 288°C, but chemical degradation occurs in steam at 316°C.[21-23] In a steam sterilization study, PEEK was found to exhibit an increase in strength and stiffness and a decrease in ductility after being subjected to 134°C steam for 1000 hours.[24] This behavior was attributed to slight increases in crystallinity and/or reductions in internal stresses. Increases in crystallinity are not favorable because it results in dimensional changes, embrittlement and reduced sealing performance of the manufactured PAEK component.

In this study, we report the effect of high temperature steam on the crystallinity and mechanical properties of PEKKs with various T/I ratios and compare to PEEK as a benchmark. Changes in the crystalline structure were characterized by DSC and WAXD, while the effect on mechanical behavior is demonstrated through flexural properties and DMA temperature sweeps. We propose to limit crystal growth during steam exposure by reducing the
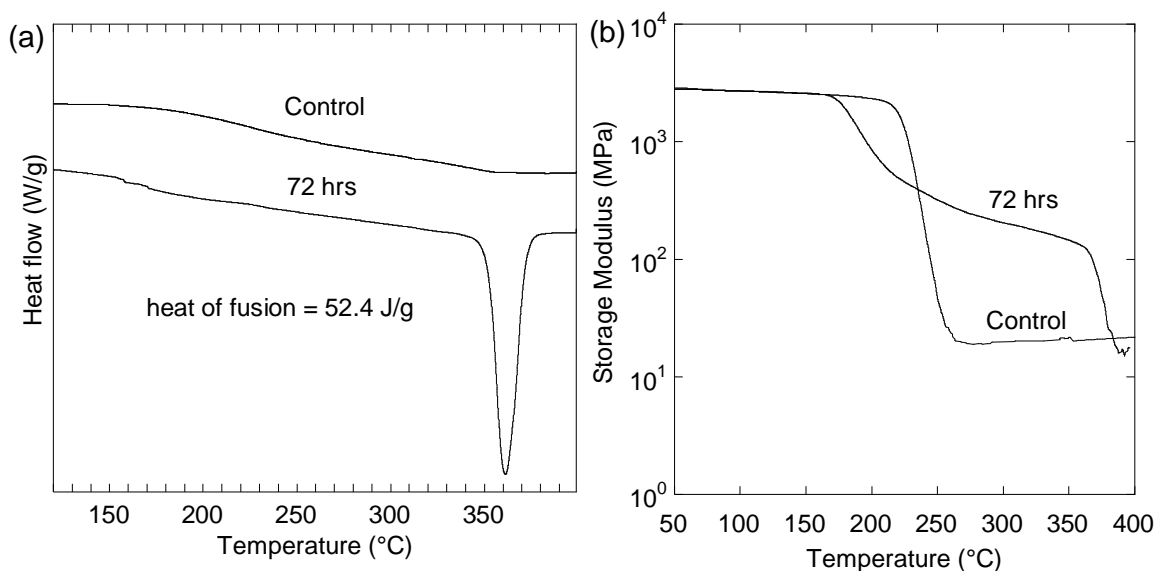
Figure 3-2. (a) DSC heating cycle thermograms and (b) temperature dependent storage modulus for ketimine crosslinked PEKK(75/25) before and after exposure to steam at 288°C for 72 hours.

polymer chain mobility through chemical crosslinking. Many methods have been reported for preparing crosslinked PAEKs through thermal annealing,[25] electron and ion irratiation[25-27] and chemical modification.[28-34] In our preliminary attempt to hinder the crystal growth in PEKK during steam exposure, we investigated the steam stability of ketimine crosslink chemistry reported previously for PEEK.[30, 31] Figure 3-2 compares the DSC heating cycle thermograms (3-2(a)) and storage moduli (3-2(b)) of ketimine crosslinked PEKK(75/25) before and after exposure to steam at 550°C for 72 hours. Before exposure to steam, it does not exhibit a melting endotherm at the expected melting temperature for neat PEKK(75/25) (~360°C). The crosslinking reaction occurs very fast at the specimen molding temperature such that this material does not develop a crystalline microstructure during cool down from the molten state. Additionally, the glassy transition occurs at a higher temperature and the plateau storage modulus is maintained well above the melting temperature of neat PEKK(75/25), which is consistent with a crosslinked network lacking any crystalline phase. Both the DSC melting endotherm and DMA viscous transition reappear after exposure to steam which demonstrates that ketimine crosslinks are not

resistant to high temperature steam and do not effectively hinder steam-assisted crystallization. Ketimine crosslinks likely hydrolyze under steam conditions to regenerate ketones present in neat PEKK(75/25).

In this work, we utilize a xanthydrol-based crosslinking chemistry for PEKK shown in Figure 3-1(c) to enhance steam resistance through crystallization control. The crosslink precursor is inspired by a well-known 9-phenylenexanthydrol end-group that can form during Friedel-Crafts polyacylation of PEKK.[35] Reaction of these end groups contributes to gelation, poor melt stability and undesirable flow characteristics in PEKK melts.[36] Through careful control of crosslinking precursor and reaction conditions we are able to effectively stabilize the crystal structure. We use DSC, WAXD and DMA to evaluate the effect of high temperature steam on both neat and xanthydrol crosslinked PAEKs.

3.2 Experimental

Polymics, Ltd. provided injection molded ASTM D638 Type I tensile specimens of PEEK, PEKK(75/25), bPEKK(88/12) and XL-PEKK(75/25). The T/I ratio of PEKK is indicated in parenthesis. PEKK(75/25) is a random copolymer and bPEKK(88/12) is a melt blend with an average T/I ratio of 88/12. XL-PEKK(75/25) is crosslinked PEKK(75/25) that was prepared using a xanthydrol crosslinking group according to a proprietary method. Ketimine crosslinked PEKK(75/25) specimens were prepared by dry mixing fine powders of phenylene diamine (10 mol% based on ketone content) and PEKK(75/25), then molding rectangular bars in a hydraulic press equipped with heated platens. All specimens were annealed at 220°C prior to steam exposure experiments.

Steam exposure was conducted in a Parr pressure reactor (Model Number 4521M) equipped with 2000 psi pressure gauge, J-type thermocouple, manual pressure relief valve and rupture disc rated for 2000 psi. The internal temperature of the reactor was maintained using a resistive heating jacket controlled by a digital microcontroller.

Reactor cylinder is charged with 200 mL of distilled water. Tensile specimens are supported as high as possible above the water level using stainless steel mesh and vertical risers. The reactor lid fitted with a PTFE gasket is installed and a 12" J-type thermocouple is secured through the center of the lid using compression fittings. The reactor is placed in a resistive heating jacket and heated up at ~3°C/min until reaching desired temperature. Steam aging time starts when reactor reaches desired temperature. Typical pressure for 288°C steam is approximately 1100 psi. After the steam aging duration, the heater is turned off and the reactor is allowed to cool under ambient conditions until pressure is 0 psig (~6 hours). Then the reactor is vented and opened to remove specimens. All specimens were dried overnight at 150°C after steam exposure to remove absorbed water before further characterization.

Three-point flexural tests were conducted with an Instron load frame (Model 3367) with 10kN load cell and 5kN flexure fixture. Lower anvil span was 50 mm and upper anvil speed was 5 mm/min.

DSC experiments were conducted with TA Instruments DSC Q20 with a programmed temperature ramp to 400°C or 450°C at 10°C/min. Thermal events and heats of fusion were determined from thermograms using TA Universal Analysis software package.

DMA experiments were conducted with TA Instruments DMA Q800 in three-point bending mode with nitrogen purge. Specimens were rectangular and measured 3x13x60mm. Typical DMA method: Equilibrate at 50°C for 5 min, oscillate at 1 Hz and 0.01% strain during temperature ramp to 400°C at 2°C/min

WAXD experiments were conducted using Rigaku D/MAX RAPID with area detector and Cu X-ray source (λ= 1.542 Å). Data collected in transmission mode. Exposure conditions were the same for all samples.

FTIR spectra were collected using Bruker Vertex V70 equipped with MVP-Pro Star Attenuated Total Reflectance (ATR) accessory (diamond crystal) from Harrick Scientific Products, Inc.

3.3 Results and Discussion

Semi-crystalline PEEK, PEKK(75/25), bPEKK(88/12) and XL-PEKK(75/25) were exposed to 288°C steam for various durations. The T/I ratio for PEKKs is shown in parenthesis. PEEK is included as the incumbent PAEK for steam handling applications. PEKK(75/25) and bPEKK(88/12) potentially can be used at higher service temperature than PEEK due to their higher T_m. PEKK(75/25) is a random copolymer, while bPEKK(88/12) is a melt blend of low and high T/I ratio PEKK (average T/I ratio of melt blend is 88/12). XL-PEKK(75/25) is semi-crystalline and contains xanthydrol-based crosslinks to stabilize the crystalline microstructure. The effects of steam exposure on the four PAEKs were evaluated using DSC, WAXD, flex testing, FTIR, and DMA.

3.3.1 Differential Scanning Calorimetry (DSC)

Changes in crystallinity upon exposure to high temperature steam were identified by monitoring the melting endotherm shape, and by integrating the melting endotherm to track heats of fusion. Figure 3-3 shows DSC thermograms obtained during the first heating cycle for (a) PEEK, (b) PEKK(75/Need 25), (c) bPEKK(88/12) and (d) XL-PEKK(75/25) after various

durations of steam exposure at 288°C. Unexposed PEEK exhibits a relatively broad melting endotherm followed by narrow double melting endotherms after 24 and 48 hours of exposure. Double melting behavior is well documented for PEEK and is thought to be melting and subsequent recrystallization of smaller, less stable lamella upon heating during a DSC experiment.[37-40] The occurrence of double-melting behavior after 24 hours suggests a new
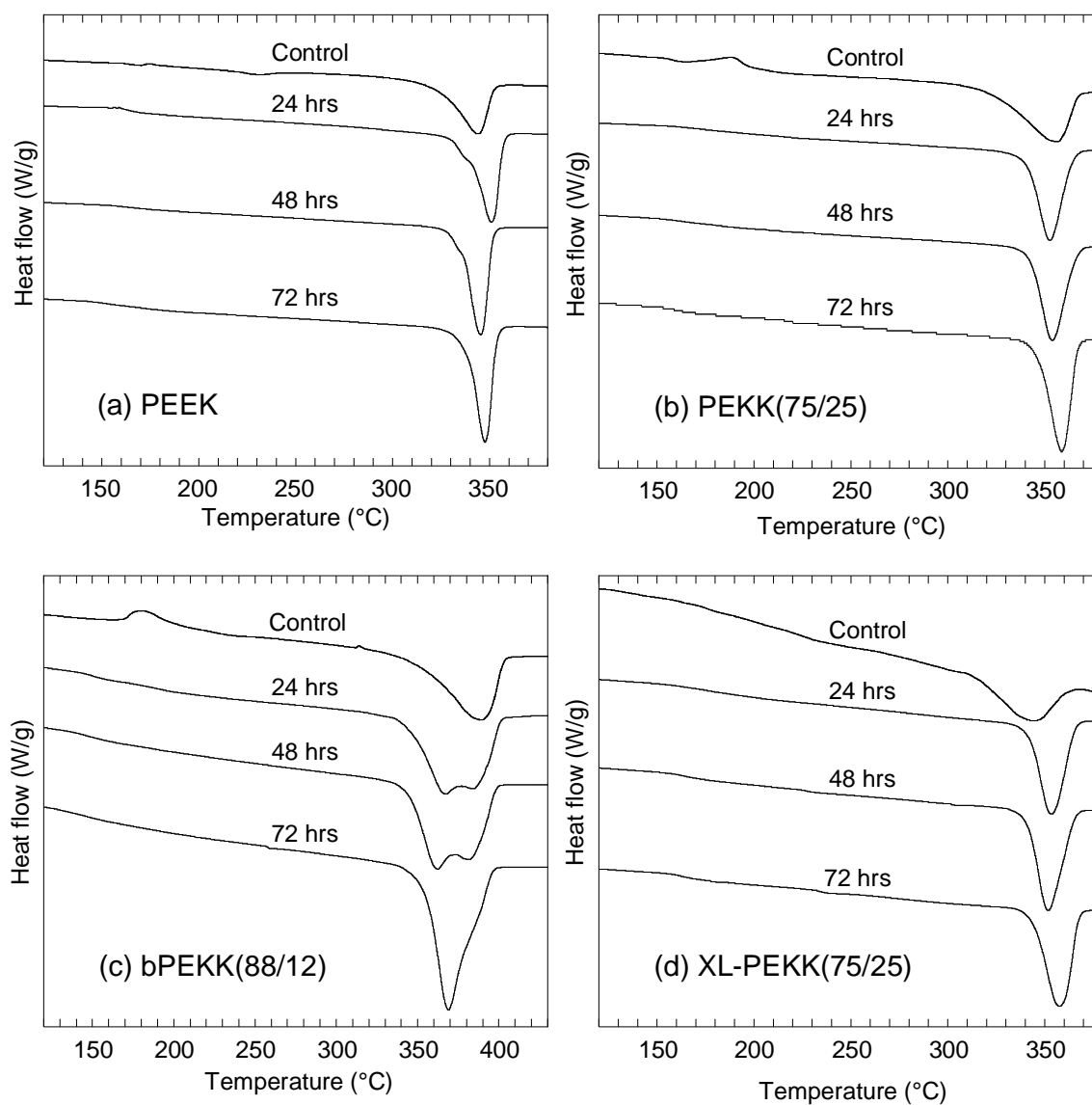
Figure 3-3: DSC curves for (a) PEEK, (b) PEKK(75/25), (c) bPEKK(88/12) and (d) XL-PEKK(75/25) after exposure to 288°C steam for 0, 24, 48 and 72 hrs.

population of small lamella forms from the amorphous phase. The lower temperature melting endotherm eventually disappears with further steam exposure and the peak shape is narrower compared to unexposed PEEK, which suggests the new smaller lamella continue to grow in the steam environment until achieving a narrow size distribution of larger crystallites.

High temperature steam also assists crystal reorganization and growth in PEKK(75/25). While PEKK(75/25) does not show double melting behavior (Figure 3-3(b)), the single melting endotherm becomes increasingly narrower and shifts to higher temperature with increased steam exposure. This is once again indicative of a narrowly distributed population of overall larger crystallites.

Unexposed bPEKK(88/12) has a single broad melting endotherm with a peak maximum at ~390°C (Figure 3-3(c)). As expected, the melting temperature is higher compared to PEKK(75/25) (~355°C) because the T/I ratio is greater. Upon exposure to steam for 24 hours, the single melting endotherm is replaced by two distinct lower temperature melting endotherms at ~370°C and ~380°C. Further exposure to steam for 48 and 72 hours causes the melting endotherm at ~380° to diminish and the melting endotherm at ~370°C to dominate. This trend is opposite of PEEK and PEKK(75/25), for which the melting endotherms shift to higher temperature with increased steam exposure. The crystal structure and thermodynamic stability of bPEKK(88/12) is likely to be more complex because it is not a random copolymer, rather a melt blend of low T/I PEKK and high T/I PEKK. We propose the melting temperature of unexposed PEKK(88/12) is closer to the melting temperature of the high T/I PEKK because its crystals are kinetically favored to contain more terephthaloyl units due to the faster crystallization rate of high T/I PEKK.[19] Upon increased steam exposure, the initial melting endotherm at ~390°C shifts to lower temperature due to incorporation of more isophthaloyl units into the existing crystalline structure. The appearance of an entirely new melting endotherm at ~370°C may correspond to new crystal growth with a T/I ratio close to the low T/I PEKK component. This reorganization

behavior is not expected to occur in PEKK(88/12) random copolymer because all of the chains theoretically have the same T/I ratio, stiffness and mobility. Furthermore, specific T/I ratios obtained by post-polymerization blending, rather than copolymerization, can potentially experience dramatic microstructural reorganization while in use, which may adversely affect maximum use temperature and service lifetime.

Initially, the melting endotherm for XL-PEKK(75/25) (Figure 3-3(d)) is broad and has its maximum at ~345°C, which is lower compared to PEKK(75/25) (~355°C). XL-PEKK(75/25) retains its semi-crystalline nature after the crosslinking reaction, which is not the case for ketamine crosslinked PEKK as discussed later. Similar to PEEK and PEKK(75/25), the melting endotherm becomes narrower and shifts to a slightly higher temperature (~360°C) upon exposure to steam. This indicates the crystallites also reorganize into larger structures with a more narrow size distribution.
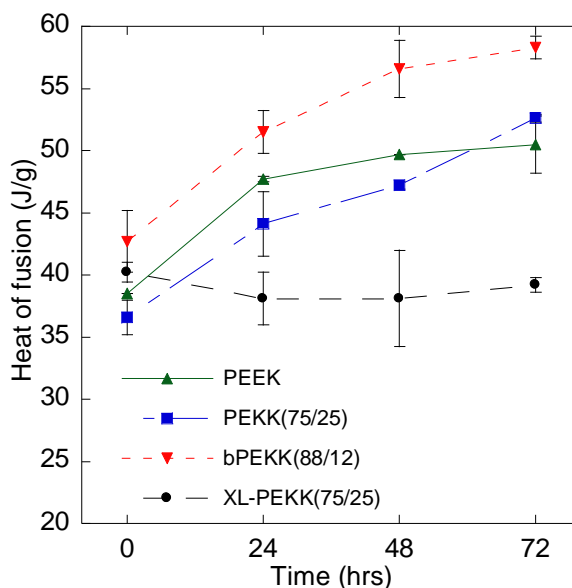
Figure 3-4: Heats of fusion for PEEK, PEKK(75/25), bPEKK(88/12) and XL-PEKK(75/25) as a function of time exposed to 288°C saturated steam. Values are obtained by integrating the melting endotherms shown in Figure 3-3. Each data point is an average of at least 2 samples and error bars represent standard deviation.

We use the heat of fusion as measured by DSC to monitor the relative change in the amount of crystalline material in each sample. The heats of fusion for each sample were calculated by integrating the area enclosed by the melting endotherm and a suitable baseline. Figure 3-4 shows the heat of fusion for (a) PEEK, (b) PEKK(75/25), (c) bPEKK(88/12) and (d) XL-PEKK(75/25) as a function of time exposed to steam at 288°C. The heats of fusion increase appreciably for PEEK, PEKK(75/25) and bPEKK(88/12), suggesting the crystalline phase fraction grows by as much as 30%, 46% and 36%, respectively, upon 72 hours of steam exposure after which the increase begins to plateau. Additionally, the change in heat of fusion and therefore degree of crystallinity is significant; the heat of fusion for 100% crystalline PEEK is 130 J/g,[41] which we speculate is a similar order of magnitude for the other PAEKs in this study. An increase in heat of fusion was not observed when the same materials were annealed at 288°C in only air, indicating that steam plays an essential role in the solvent-assisted crystallization of these PAEK materials. In contrast, the heat of fusion of XL-PEKK(75/25) does not change appreciably after steam exposure for up to 72 hours. This crosslinking chemistry appears to be stable in high temperature steam and achieves the anticipated effect of preventing additional crystallization. The change in the position and shape of the melting endotherms in Figure 3-3(d) however, suggests the crystallites are generally larger after steam exposure.

3.3.2 Wide-Angle X-ray Diffraction (WAXD)

WAXD was used to observe changes in the crystal structure and to determine degree of crystallinity. Figure 3-5 shows one-dimensional WAXD data for (a) PEEK, (b) PEKK(75/25), (c) bPEKK(88/12) and (d) XL-PEKK(75/25) after various durations of exposure to steam at 288°C. The WAXD data obtained for unexposed PEEK and PEKK(75/25) is comparable to reported literature, which cites an orthorhombic crystal lattice.[42] PEEK shows improved resolution of all diffraction peaks and a reduction in the broad amorphous scattering peak from $q = 1.0$ to 1.3 Å^{-1}

with increasing steam exposure. This is consistent with growth of the crystalline phase supported by DSC experiments and the increase in crystallinity determined from WAXD data demonstrated in Figure 3-6. PEKK(75/25) and bPEKK(88/12) show similar behavior to PEEK and are consistent with increases in crystallinity observed by DSC and WAXD.

bPEKK(88/12) exhibits diffraction peaks characteristic of both accepted polymorphs of PEKK referred to in the literature as form I and form II. Form I is the more stable structure and has a two-chain orthorhombic unit cell with chains located at the corners and center of the unit cell.[19] Form II is characterized by a one-chain orthorhombic unit cell with chains at the corners of
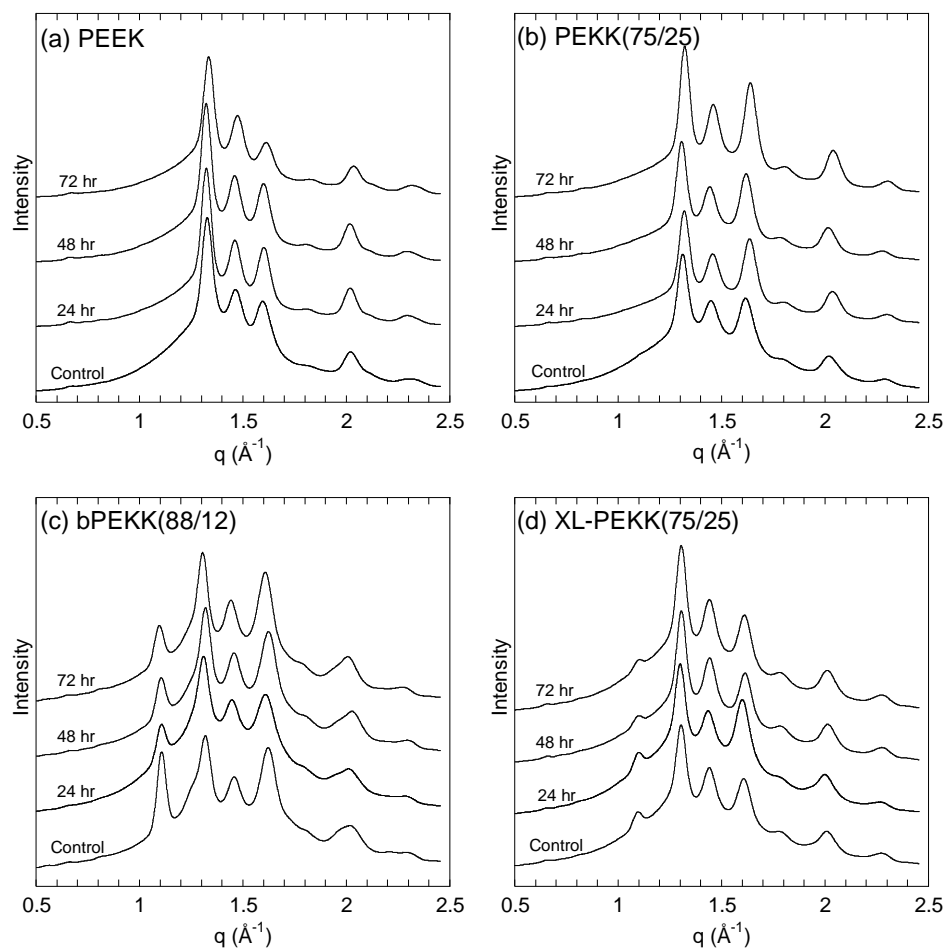
Figure 3-5: WAXD data for (a) PEEK, (b) PEKK(75/25), (c) bPEKK(88/12) and (d) XL-PEKK(75/25) after exposure to 288°C steam for 0, 24, 48 and 72 hrs.

the unit cell.[43] The form II structure is favored under diffusion-limited conditions, such as crystallization from the melt at high supercoolings,[44] and during thermal and solvent-induced crystallization from the amorphous state.[45] bPEKK(88/12) has a diffraction peak at $q = 1.1$ $\mathring{A}^{-1}$, which is assigned to the (020) plane of the less thermodynamically stable form II structure. The ability to crystallize in the form II structure has been observed to increase with increasing chain stiffness and decreasing chain mobility, which is achieved through a higher T/I ratio.[46] Form II likely formed in bPEKK(88/12) because the initial crystalline structure consists mainly of the high T/I PEKK component. Increased exposure to high temperature steam reduces the intensity of this characteristic diffraction peak because the steam assists growth and reorganization to the thermodynamically favored form I polymorph.

The WAXD data for XL-PEKK(75/25) indicates it is comprised at least partially of form II even though PEKK(75/25) is exclusively form I. This is probably due to the formation of a small number of crosslinks during melt processing, which reduces chain mobility during crystallization. Figure 3-6 shows the crystallinity of XL-PEKK(75/25) determined from WAXD data does not increase significantly with increasing steam exposure and is consistent with the minimal change in heat of fusion observed by DSC. This finding supports our hypothesis that crosslinking of the amorphous region can inhibit additional crystal growth.
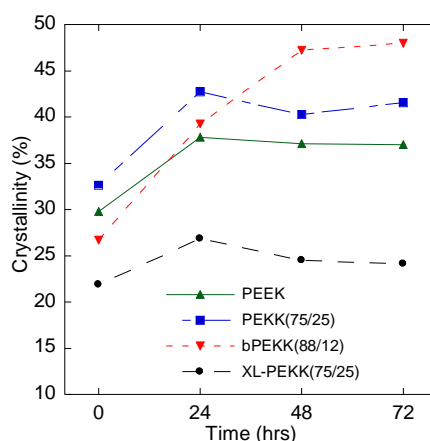
Figure 3-6: Crystallinity from WAXD data of PEEK, PEKK(75/25), bPEKK(88/12) and XL-PEKK(75/25) as a function of time aged in 288°C saturated steam.

3.3.3 Flexural Properties

Flexural properties were measured to probe the effect of crystalline microstructural changes after steam exposure. Figure 3-7 contains the flexural stress-strain curves for (a) PEEK, (b) PEKK(75/25), (c) bPEKK(88/12) and (d) XL-PEKK(75/25) after various durations of exposure to steam at 288°C. PEEK is generally more ductile compared to semi-crystalline PEKK(T/I). The slope of the stress-strain curve (flexural modulus) and yield strength increase with increasing exposure to steam, which is owed to the significant growth of the crystalline
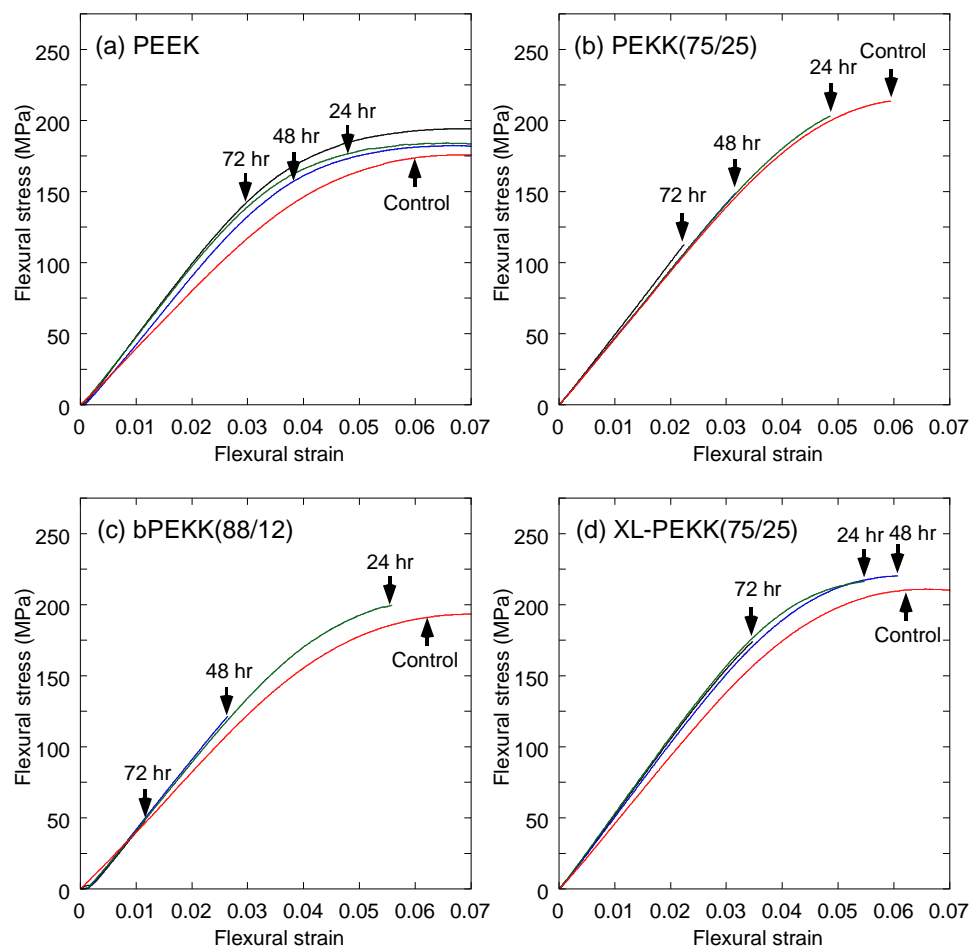
Figure 3-7: Flexural stress vs. strain for (a) PEEK, (b) PEKK(75/25), (c) bPEKK(88/12) and (d) XL-PEKK(75/25) after exposure to 288°C saturated steam for various times. All tests were stopped at a maximum flexural strain of 0.07.

phase observed in DSC and WAXD experiments. The crystal growth does not have an effect on the ductility of PEEK probably due to the superior chain flexibility of additional ether bonds compared to PEKK(T/I). Semi-crystalline PEKK(75/25) and bPEKK(88/12) are both less ductile than PEEK and suffer from embrittlement with increasing exposure to steam as shown in Figure 3-7(b). We attribute the reduction in mechanical properties to crystalline microstructural changes rather than chemical degradation. Figure 3-8 compares the surface FTIR spectra of (a) PEEK, (b) PEKK(75/25), (c) bPEKK(88/12) and (d) XL-PEKK(75/25) for unexposed samples and samples exposed to steam for 72 hours at 288°C. Despite differences in absorption intensities due to variable specimen contact with the ATR crystal, there is no evidence of significant chemical degradation in any of the materials.
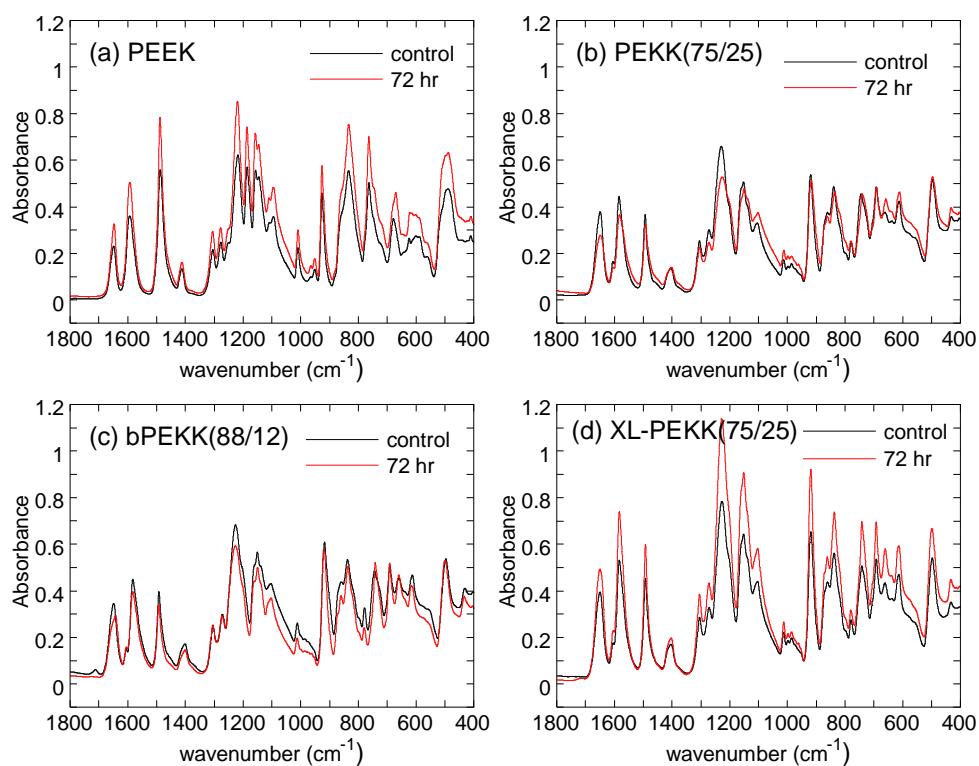
Figure 3-8: FTIR spectra of (a) PEEK, (b) PEKK(75/25), (c) bPEKK(88/12) and (d) XL-PEKK(75/25) before (control) and after exposure to 288°C steam for 72 hours.

The flexural modulus and strength of XL-PEKK(75/25) initially increase after 24 hours of exposure to steam similar to PEEK. Although embrittlement is still observed, the retention of strength is improved compared to PEKK(75/25) and bPEKK(88/12). Figure 3-9 compares the yield strength of all the materials as a function of time exposed to steam at 288°C. PEEK clearly has the best retention of flexural strength, while PEKK(75/25) and bPEKK(88/12) rapidly lose strength due to embrittlement after 24 hours. In contrast, the data from XL-PEKK(75/25) exemplify a significant improvement until 48 hours after which the decrease in flexural strength occurs at a rate comparable to PEKK(75/25) and bPEKK(88/12).
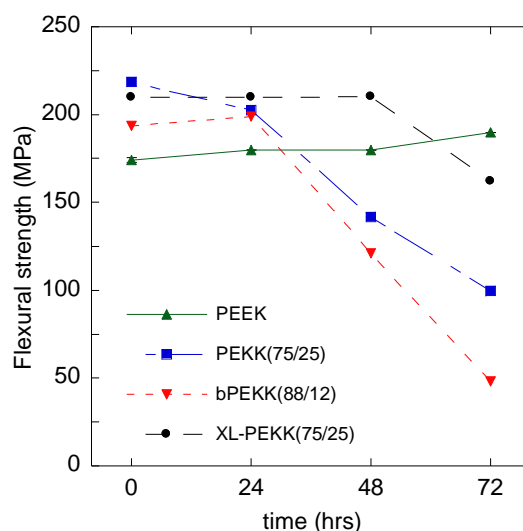
Figure 3-9: Flexural strength (from Figure 3-7) of PEEK, PEKK(75/25), bPEKK(88/12) and XL-PEKK(75/25) as a function of time exposed to 288°C steam.

Because the degree of crystallinity for XL-PEKK(75/25) does not change over the entire exposure time range, the observed embrittlement may be caused by reorganization of smaller crystals into larger ones as suggested by narrowing of the melting endotherm in Figure 3-3. We speculate that PAEKs and other semicrystalline rigid polymers with larger crystallites formed at low supercoolings (nucleation-limited) exhibit higher strength and lower ductility compared to specimens with smaller crystallites formed at high supercoolings (diffusion-limited).[47, 48]

Figure 3-10: DMA specimens of (a) PEEK and (b) XL-PEKK(75/25) after temperature ramp to 400°C.

A semicrystalline morphology with smaller crystals formed under diffusion-limited conditions could lead to less brittle materials due to greater tie chain densities.[49]

Although PEEK retains a higher strength after 72 hrs of steam exposure, the material becomes soft at elevated temperatures. Figure 3-10 shows that PEEK deforms significantly at 350°C, while XL-PEKK(75/25) does not. This highlights the advantage of dimensional stability at high temperatures, even after steam exposure, of XL-PEKK(75/25). We further explore the mechanical properties of PAEKs using dynamic mechanical analysis, as discussed below.

3.3.4 Dynamic Mechanical Analysis (DMA)

DMA in three-point bending mode was used to probe the high temperature properties of specimens before and after exposure to high temperature steam. Figure 3-11 shows the storage modulus curves obtained during a temperature sweep of (a) PEEK, (b) PEKK(75/25), (c) bPEKK(88/12) and (d) XL-PEKK(75/25) after various durations of exposure to steam at 288°C. The rubbery plateau storage modulus for PEEK, PEKK(75/25) and bPEKK(88/12) increase with increasing steam exposure, which is due to the observed increase in degree of crystallinity. A clear transition to viscous behavior and loss of dimensional stability occurs for all of these materials near their melting temperature as measured by DSC. XL-PEKK(75/25) exhibits a similar transition near its melting point, but retains some elastic character and dimensional

stability up to 400°C even after steam exposure as evident from the finite storage modulus plateau above ~375°C. This is further evidence that the crosslinked structure is stable in a high temperature steam environment.
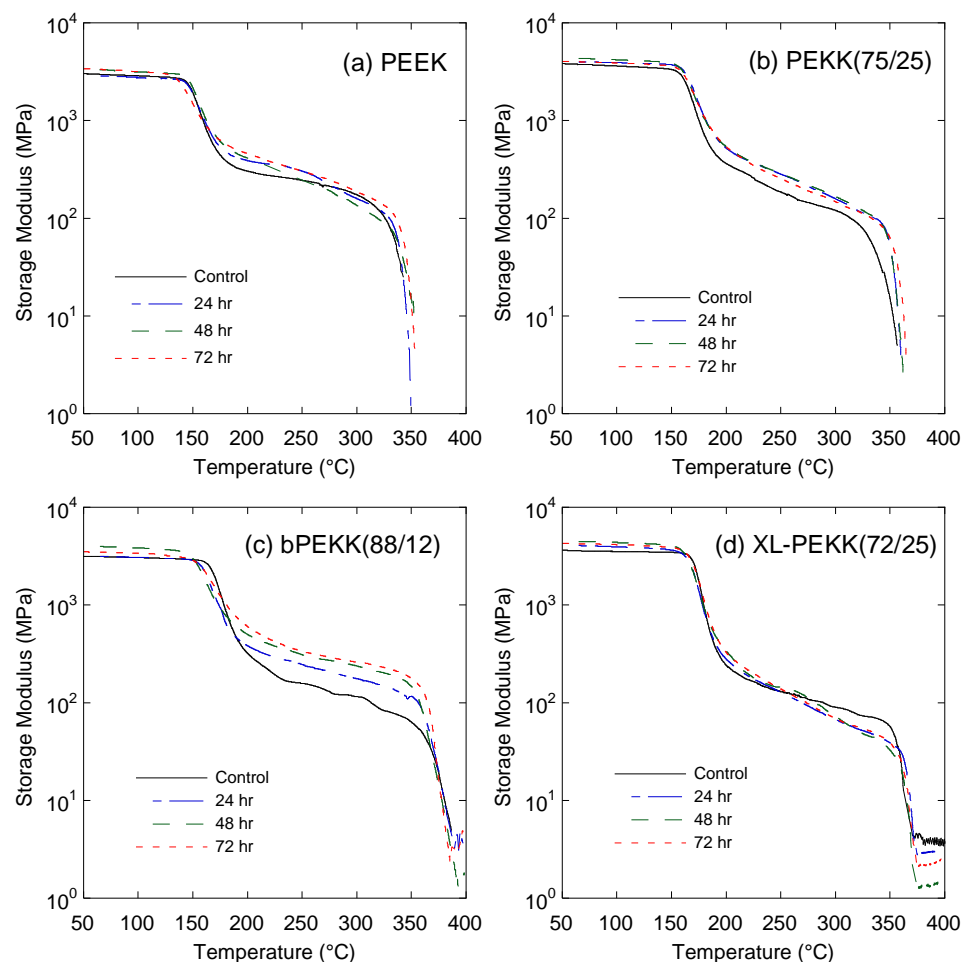
Figure 3-11: DMA curves for (a) PEEK, (b) PEKK(75/25), (c) bPEKK(88/12) and (d) XL-PEKK(75/25) aged in 288°C saturated steam for various times. XL-PEKK(75/25) retains a finite modulus at high temperatures.

3.4 Conclusions

PAEKs are potentially well-suited for handling and containing high pressure, high temperature steam used in steam-assisted oil recovery technologies due to their thermal and hydrolytic stability. Current PAEK materials typically suffer from embrittlement due to steam-

assisted crystallization at temperatures greater than the glass transition, which reduces the lifetime of fabricated seals and back-up rings. We demonstrated high temperature steam (288°C) has an annealing effect on currently available PEEK and PEKK(T/I), and results in further crystallization and rearrangement of existing phases into thermodynamically favorable crystalline phases in the case of polymorphic PEKK(T/I). Crystal growth is detrimental to the performance of manufactured parts because it causes embrittlement and dimensional changes that contribute to short lifetime and reduced seal performance.

We used xanthydrol-based crosslinking chemistry to stabilize the PEKK crystal structure in order to reduce steam-assisted crystallization. Xanthydrol crosslinks are significantly more stable in high temperature steam compared to legacy ketimine crosslinking chemistry and they effectively limit steam-assisted crystallization. Crosslinked PEKK maintains its degree of crystallinity and exhibits better retention of mechanical properties after steam exposure compared to neat PEKK(75/25). Additionally, xanthydrol-crosslinked PEKK can be prepared as a semi-crystalline material, which improves high temperature creep resistance for sealing applications. Future advances in steam resistant PAEKs include crosslinking strategies that can further stabilize the PEKK crystal structure in order to prevent crystallite growth due to steam-assisted annealing.

3.5 References

1. Steinberg, E. L., Rath, E., Shlaifer, A., Chechik, O., Maman, E. and Salai, M. *Journal of the Mechanical Behavior of Biomedical Materials* **2013**, 221-228.
2. Nakahara, I., Takao, M., Bandoh, S., Bertollo, N., Walsh, W. R. and Sugano, N. *Journal of Orthopaedic Research* **2013**, *3*, 485-492.
3. Lee, K. S., Shin, M. S., Lee, J. Y., Ryu, J. J. and Shin, S. W. *Journal of Advanced Prosthodontics* **2017**, *5*, 350-357.
4. Diaz, G., Sampurno, Y. and Philipossian, A. *Ecs Journal of Solid State Science and Technology* **2018**, *9*, P447-P451.

5. Liao, X., Sampurno, Y., Zhuang, Y., Rice, A., Sudargho, F., Philipossian, A. and Wargo, C. *Microelectronic Engineering* **2012**, 70-73.

6. Green, S., Ferfecki, F. J. and Marburger, U. *Sampe Journal* **2018**, *3*, 22-29.

7. Tan, W. and Falzon, B. G. *Composites Science and Technology* **2016**, 60-77.

8. Mazur, R. L., Botelho, E. C., Costa, M. L. and Rezende, M. C. *Polimeros-Ciencia E Tecnologia* **2008**, *3*, 237-243.

9. Mazur, R. L., Oliveira, P. C., Rezende, M. C. and Botelho, E. C. *Journal of Reinforced Plastics and Composites* **2014**, *8*, 749-757.

10. Derisi, B., Hoa, S. O. V., Xu, D., Hojjati, M. and Fews, R. *Journal of Thermoplastic Composite Materials* **2011**, *1*, 29-49.

11. Weidig, R. and GmbH, V. D. I. W. In International Conference on Gears 2017/ International Conference on Gear Production/ International Conference on High Performance Plastic Gears 2017, Vols 1 and 2; Eds.; **2017**; Vol. 2294, pp 1565-1574.

12. Garzon-Hernandez, S., Garcia-Gonzalez, D. and Arias, A. *Composite Structures* **2018**, 241-252.

13. Lan, P. X., Meyer, J. L., Vaezian, B. and Polycarpou, A. A. *Wear* **2016**, 10-20.

14. Lan, P. X. and Polycarpou, A. A. *Tribology International* **2018**, 218-225.

15. Xu, A. Z., Mu, L. X., Fan, Z. F., Wu, X. H., Zhao, L., Bo, B. and Xu, T. *Journal of Petroleum Science and Engineering* **2013**, 197-207.

16. Liu, P. C., Zheng, H. M. and Wu, G. H. *Journal of Energy Resources Technology-Transactions of the Asme* **2017**, *1*,

17. Bao, Y., Wang, J. Y. and Gates, I. D. *Journal of Petroleum Science and Engineering* **2017**, 268-282.

18. Veazey, D., Hsu, T. and Gomez, E. D. *Journal of Applied Polymer Science* **2017**, *6*, 44441.

19. Gardner, K. H., Hsiao, B. S., Matheson, R. R. and Wood, B. A. *Polymer* **1992**, *12*, 2483-2495.

20. S., H. B., H., G. K. and D., C. S. Z. *Journal of Polymer Science Part B: Polymer Physics* **1994**, *16*, 2585-2594.

21. Pope, J. C., Sue, H.-J., Bremner, T. and Bluemel, J. *Journal of Applied Polymer Science* **2015**, *6*, 41421.

22. Pope, J. C., Sue, H. J., Bremner, T. and Blumel, J. *Polymer* **2014**, *18*, 4577-4585.

23.   Guenther, J., Wong, M. H., Sue, H. J., Bremner, T. and Blumel, J. *Journal of Applied Polymer Science* **2013**, *6*, 4395-4404.

24.   Green, S. and Cartwright, K. The Resistance of PEEK-OPTIMA® Polymer to High Temperature Autoclave Sterilisation. Report Number 004003, May 2004.

25.   Al Lafi, A. G., Parker, D. J. and Hay, J. N. *Journal of Applied Polymer Science* **2015**, *22*,

26.   Sasuga, T. and Kudoh, H. *Polymer* **2000**, *1*, 185-194.

27.   Vaughan, A. S. and Stevens, G. C. *Polymer* **2001**, *21*, 8891-8895.

28.   He, Q. Z., Wang, J. Y., Zong, L. S., Liu, R. and Jian, X. G. *Polymer International* **2015**, *7*, 875-883.

29.   Hendrix, K., Van Eynde, M., Koeckelberghs, G. and Vankelecom, I. F. J. *Journal of Membrane Science* **2013**, 212-221.

30.   Yurchenko, M. E., Huang, J. J., Robisson, A., McKinley, G. H. and Hammond, P. T. *Polymer* **2010**, *9*, 1914-1920.

31.   Tu, H. and Robisson, A. (Schlumberger Technology Corporation). U.S. Patent 8,436,106, May 7, 2013.

32.   Thompson, S. A. and Farris, R. J. *Journal of Applied Polymer Science* **1988**, *5*, 1113-1120.

33.   Brugel, E., David, I. and Gay, F. (E.I. Du Pont de Nemours and Company). U.S. Patent 5,175,218, December 29, 1992.

34.   Burgoyne, W. F. J., Nordquist, A. F., Drake, K. A. and Song, L. (Greene, Tweed & Co.). U.S. Patent 9,006,353, April 14, 2015.

35.   Melissen, S., Tognetti, V., Dupas, G., Jouanneau, J., Le, G. and Joubert, L. *Journal of Molecular Modeling* **2016**, *1*, 14.

36.   Angelo, R. J., Darms, R. and Wysong, R. D. (E. I. du Pont de Nemours and Company). U.S. Patent 3,767,620, October 23, 1973.

37.   Lee, Y. and Porter, R. S. *Macromolecules* **1987**, *6*, 1336-1341.

38.   Lee, Y. C., Porter, R. S. and Lin, J. S. *Macromolecules* **1989**, *4*, 1756-1760.

39.   Ji, X. L., Zhang, W. J. and Wu, Z. W. *Journal of Polymer Science Part B-Polymer Physics* **1997**, *3*, 431-436.

40.   Velikov, V. and Marand, H. *Abstracts of Papers of the American Chemical Society* **1993**, 324-POLY.

41.   Blundell, D. J. and Osborn, B. N. *Polymer* **1983**, *8*, 953-958.

42.   Dawson, P. C. and Blundell, D. J. *Polymer* **1980**, *5*, 577-578.

43. Ho, R. M., Cheng, S. Z. D., Hsiao, B. S. and Gardner, K. H. *Macromolecules* **1994**, *8*, 2136-2140.

44. Choupin, T., Fayolle, B., Regnier, G., Paris, C., Cinquin, J. and Brule, B. *Polymer* **2017**, 73-82.

45. Cheng, S. Z. D., Ho, R. M., Hsiao, B. S. and Gardner, K. H. *Macromolecular Chemistry and Physics* **1996**, *1*, 185-213.

46. Gardner, K. H., Hisao, B. S. and Faron, K. L. *Polymer* **1994**, *11*, 2290-2295.

47. Yang, C. C., Tian, X. Y., Li, D. C., Cao, Y., Zhao, F. and Shi, C. Q. *Journal of Materials Processing Technology* **2017**, 1-7.

48. Talbott, M. F., Springer, G. S. and Berglund, L. A. *Journal of Composite Materials* **1987**, *11*, 1056-1081.

49. Vakhshouri, K. and Gomez, E. D. *Macromolecular Rapid Communications* **2012**, *24*, 2133-2137.

Chapter 4

Summary and Recommendations for Future Work

4.1 Summary

The excellent mechanical properties and chemical resistance of PAEKs make them good candidates for oil and gas sealing and compressor applications where high temperatures and pressures and corrosive fluids are frequently encountered. For example, steam assisted gravity drainage and cyclic steam injection utilize high temperature steam (up to 340°C) to heat and extract heavy crude oil from oil sands formations. Steam resistance is particularly challenging for PAEKs, however, due to the steam-assisted crystallization that occurs. In situ crystallization causes dimensional changes and embrittlement, which shorten service lifetime and increase the risk of pipeline leakage or machinery failure.

The original research presented in this thesis evaluates the effect of high temperature steam on various neat and modified PAEKs. As expected, the neat PAEKs in this study experienced steam-assisted crystallization in the presence of high temperature steam above the T_g. PEEK, PEKK copolymers and PEKK melt blends experience an increase in degree of crystallinity much greater than that obtained by quiescent crystallization from the molten state. DSC results suggest the smaller crystallites grow larger and the crystallite size distribution becomes narrower overall. The increase in crystallinity was typically accompanied by embrittlement and reduced strength. Additionally, the initial T_m of the melt blended PEKK is quite high as expected due to the average high T/I ratio. The T_m of the melt blended PEKK apparently decreases upon steam exposure because the low T/I ratio amorphous region forms a lower T_m crystalline phase. This suggests that crystalline microstructures of neat PEKK melt blends are not thermodynamically stable and precautions should be taken if the material is to be used in environments where in situ annealing or crystallization might occur.

Crosslinking of the amorphous region is proposed to prevent steam-assisted crystallization by effectively stabilizing the semicrystalline microstructure. Crosslinks are thought to restrict the mobility of polymer chains in the amorphous phase thereby preventing them from crystallizing even in the presence of steam. Ketimine crosslinks (C=N-C bond) at the ketone positions did not prevent further crystallization and were likely completely hydrolyzed upon exposure to steam. In contrast, xanthydrol-based crosslinks (C-C bond) prevented an increase in the degree of crystallinity and improved the strength retention compared to neat PAEK. Additionally, the crosslinked PEKK developed as part of this work exhibits good dimensional stability and retains elastic behavior above the T_m, which is a significant improvement over existing conventional PAEKs.

4.2 Recommendations for Future Work

Further improvements to the steam resistance of PAEKs are still necessary in order to increase their service life and reduce the risk of machinery failure. While the xanthydrol crosslink chemistry proves to be stable in high temperature steam and effectively inhibits formation of additional crystallites, the existing small crystallites apparently experience some degree of growth or reorganization into larger crystallites. As discussed in chapter 3, existence of larger crystallites may contribute to embrittlement due to the lower number of tie chains between them. Furthermore, tie chain density may be preserved through stabilization of the existing crystalline phase, especially smaller crystallites. Greater crosslink densities or shorter crosslinks may achieve this by restricting chain motion to a greater extent at the crystalline-amorphous interface where growth is expected to occur. Future work should focus on the design and synthesis of short chain xanthydrol-based crosslink precursors and PAEK materials that incorporate them at various concentrations. Subsequently, the resultant crosslinked PAEKs should be evaluated for their resistance to all steam-assisted crystallization.